Cell

Somatic Mutations of the Immunoglobulin Framework Are Generally Required for Broad and Potent HIV-1 Neutralization

Florian Klein,[1,12] Ron Diskin,[3,5,12] Johannes F. Scheid,[1,6] Christian Gaebler,[1,7] Hugo Mouquet,[1] Ivelin S. Georgiev,[8] Marie Pancera,[8] Tongqing Zhou,[8] Reha-Baris Incesu,[1,9] Brooks Zhongzheng Fu,[3] Priyanthi N.P. Gnanapragasam,[3] Thiago Y. Oliveira,[1,10] Michael S. Seaman,[11] Peter D. Kwong,[8] Pamela J. Bjorkman,[3,4,13] and Michel C. Nussenzweig[1,2,13,*]

[1]Laboratory of Molecular Immunology
[2]Howard Hughes Medical Institute
The Rockefeller University, New York, NY 10065, USA
[3]Division of Biology
[4]Howard Hughes Medical Institute
California Institute of Technology, 1200 E. California Boulevard, Pasadena, CA 91125, USA
[5]Department of Structural Biology, Weizmann Institute of Science, Rehovot 76100, Israel
[6]Charité Universitätsmedizin, D-10117 Berlin, Germany
[7]Faculty of Medicine Carl Gustav Carus, Technische Universität Dresden, D-01307 Dresden, Germany
[8]Vaccine Research Center, National Institute of Allergy and Infectious Diseases, National Institutes of Health (NIH), Bethesda, MD 20892, USA
[9]Universitätsklinikum Hamburg-Eppendorf, D-20246 Hamburg, Germany
[10]Department of Genetics, Medical School of Ribeirao Preto/USP, National Institute of Science and Technology for Stem Cells and Cell Therapy and Center for Cell-based Therapy, Ribeirao Preto, SP 14051–140, Brazil
[11]Beth Israel Deaconess Medical Center, Boston, MA 02215, USA
[12]These authors contributed equally to this work
[13]These authors contributed equally to this work
*Correspondence: nussen@rockefeller.edu
http://dx.doi.org/10.1016/j.cell.2013.03.018

SUMMARY

Broadly neutralizing antibodies (bNAbs) to HIV-1 can prevent infection and are therefore of great importance for HIV-1 vaccine design. Notably, bNAbs are highly somatically mutated and generated by a fraction of HIV-1-infected individuals several years after infection. Antibodies typically accumulate mutations in the complementarity determining region (CDR) loops, which usually contact the antigen. The CDR loops are scaffolded by canonical framework regions (FWRs) that are both resistant to and less tolerant of mutations. Here, we report that in contrast to most antibodies, including those with limited HIV-1 neutralizing activity, most bNAbs require somatic mutations in their FWRs. Structural and functional analyses reveal that somatic mutations in FWR residues enhance breadth and potency by providing increased flexibility and/or direct antigen contact. Thus, in bNAbs, FWRs play an essential role beyond scaffolding the CDR loops and their unusual contribution to potency and breadth should be considered in HIV-1 vaccine design.

INTRODUCTION

A fraction of HIV-1-infected individuals mount a broadly neutralizing serologic response (Doria-Rose et al., 2010; Simek et al., 2009) 2–3 years after infection (Mikell et al., 2011). Antibodies generated by these individuals are of great interest for vaccine design because they can protect macaques from infection (Mascola et al., 2000; Moldt et al., 2012; Shibata et al., 1999). Moreover, combinations of broadly neutralizing antibodies can control an established HIV-1 infection in humanized mice (Klein et al., 2012b).

Despite their potential importance to vaccine development and HIV-1 therapy, little was known about the molecular composition of the human anti-HIV-1 antibody response until single-cell antibody cloning techniques were developed and used for characterizing IgGs from the sera of HIV-1-infected individuals with broadly neutralizing activity (Scheid et al., 2009a; Scheid et al., 2009b). This analysis revealed highly potent bNAbs, all of which might eventually be used in vaccine development (Corti et al., 2010; Huang et al., 2012; Morris et al., 2011; Mouquet et al., 2012; Scheid et al., 2011; Walker et al., 2009, 2011b; Wu et al., 2010).

A surprising observation was that anti-HIV-1 antibodies are highly somatically mutated when compared to other immunoglobulins (IgGs) cloned from the same patients (Scheid et al., 2009a; Xiao et al., 2009a, 2009b). Whereas most human

antibodies that have undergone affinity maturation carry 15–20 V_H-gene somatic mutations (Tiller et al., 2007), potent broadly neutralizing antibodies carry 40–100 V_H-gene mutations (Corti et al., 2010; Scheid et al., 2011; Walker et al., 2009, 2011b; Wu et al., 2010; Xiao et al., 2009a, 2009b). These mutations are essential because reversion to the antibody germline sequence drastically reduces neutralizing potency and breadth (Mouquet et al., 2010; Scheid et al., 2011; Wu et al., 2011; Xiao et al., 2009b; Zhou et al., 2010). However, why so many mutations appear to be required is not known.

Wu and Kabat first divided antibody variable regions into complementarity determining regions (CDRs) and framework regions (FWRs) based on the number of somatic hypermutations in these regions (Wu and Kabat, 1970) (Figures 1A and 1B). The CDRs consist primarily of loops that form the sites of contact between the antibody and antigen (Amzel and Poljak, 1979) and account for the specificities of most antibody molecules as demonstrated by CDR grafting experiments (Jones et al., 1986). The structural integrity of the variable domains is maintained by the FWRs, which encode nine antiparallel β strands arranged into two β sheets (one sheet containing strands A, B, E, and D and the other containing strands C,'' C', C, F and G; Figures 1A and 1B). The relatively invariant β strands of the FWRs serve as a scaffold for three CDR loops, which connect strands B and C, C' and C,'' and F and G (Figures 1A and 1B) (Amzel and Poljak, 1979).

Somatic mutations are preferentially found in the CDR loops where they can alter the antibody combining site without affecting the overall structure of the variable domain (Wu and Kabat, 1970). Mutations in the FWR are usually poorly tolerated and generally biased to neutral substitutions to avoid changes that would destroy the structural underpinnings of the variable domain (Reynaud et al., 1995; Wagner et al., 1995).

Here we examine the role of somatic mutations in the development of broadly neutralizing anti-HIV-1 antibodies. In contrast to most other antibodies, including anti-HIV-1 antibodies with limited neutralization activity, we found that FWR mutations, including noncontact residues, are essential for the neutralizing activity of most potent bNAbs. We propose that the requirement to alter the FWR, without destroying its essential structural elements, accounts for the high mutation load found in broadly neutralizing anti-HIV-1 antibodies and possibly for the difficulty and prolonged latency with which such antibodies develop.

RESULTS

Somatic Hypermutation in HIV-1-Neutralizing Antibodies

To examine the role of somatic hypermutations in anti-HIV-1 antibody neutralization breadth and potency, we selected a group of 9 HIV-1-reactive antibodies with activity limited to easy to neutralize (Tier 1) HIV-1 strains (Seaman et al., 2010), and 17 antibodies with broad neutralization activity (Figures 1C and S1 and Table S1 available online). The antibodies with limited neutralizing activity included antibodies recognizing the CD4-binding site (CD4bs; 6-187, 9–913, and 11–989) (Mouquet et al., 2011; Scheid et al., 2009a), the core epitope (1–479, 2–491, and 11–591) (Mouquet et al., 2011; Pietzsch et al., 2010; Scheid et al., 2009a), the V3-loop (447-52D and 10–188) (Gorny et al., 1993; Mouquet et al., 2011), and the CD4-induced site (17b) (Thali et al., 1993) (Table S1). Eight of the 17 bNAbs also recognize the CD4bs (VRC01, NIH45-46, 3BNC60, 12A12, 1NC9, 8ANC131, 12A21, and 3BNC117) (Scheid et al., 2011; Wu et al., 2010), whereas others recognized the V1/V2 loop (PG16) (Walker et al., 2009), carbohydrates (2G12) (Calarese et al., 2003; Trkola et al., 1996), the core epitope (HJ16) (Corti et al., 2010), the base of the V3-loop (10-1074 and PGT128) (Mouquet et al., 2012; Walker et al., 2011a), the membrane proximal external region (MPER; 4E10 and 2F5) (Buchacher et al., 1994; Muster et al., 1993) and two antibodies (3BC176 and 8ANC195) (Klein et al., 2012a; Scheid et al., 2011) for which the precise epitopes are not yet determined (Figure 1C and Table S1).

Antibodies with limited neutralizing activity differ from bNAbs in that they generally carry fewer somatic mutations (Figures 1C and S1 and Table S1). We used the well-accepted Kabat system (Wu and Kabat, 1970) that utilizes sequence comparisons for FWR/CDR assignments. However, direct comparisons between Kabat and the IMGT numbering system (Giudicelli et al., 2006) (Figure 1B), which includes antibody structural data, were also performed for a subset of antibodies.

Complete reversion of somatic mutations in the heavy and light chain V genes (FWR1-3 and CDR1/2) drastically reduces anti-HIV-1 antibody binding and neutralization activity (Buchacher et al., 1994; Mouquet et al., 2010; Scheid et al., 2011; Xiao et al., 2009b; Zhou et al., 2010). Moreover, reverting only the CDR1 and CDR2 in 3BNC60 and NIH45-46 strongly diminished binding and neutralization (Figure S2A and Data S1A). To determine the functional consequences of FWR mutations, we reverted the framework residues to their germline counterparts (FWR-GL) in each of the 26 selected antibodies (Data S1B–1D) and evaluated binding to the HIV-1 envelope protein as well as their neutralization activities.

HIV-1-Reactive Antibodies with Limited Activity

As expected, reversion of somatic mutations in the FWR residues (FWR-GL) of the HIV-1 antibodies with limited breadth had only minimal effects on binding of most of these antibodies to $gp140^{YU2}$ (Figure S2B) as measured by ELISA and confirmed by surface plasmon resonance (SPR) (data not shown). Only two of these FWR-GL antibodies (9-913 and 10-188) showed a decrease in binding (Figure S2B). In agreement with the ELISA and SPR experiments, we found little or no change in neutralizing activity in most of the FWR-GL antibodies with limited neutralization activity on a panel of up to six Tier 1 viruses representing clades A, B, and C (Figure S2B and Table S2). Only antibodies 9-913 and 10-188, which displayed decreased binding to $gp140^{YU2}$, showed a decrease (9-913) or complete loss (10-188) in neutralizing activity (Figure S2B and Table S2). We conclude that with two exceptions out of nine antibodies tested, FWR mutations do not alter the binding or neutralizing activity of anti-HIV-1 antibodies with limited neutralizing activity. Thus, despite their significantly higher levels of somatic mutation, HIV-1-neutralizing antibodies with limited breadth resemble previously characterized antibodies to other antigens in that FWR mutations seem not to be essential.

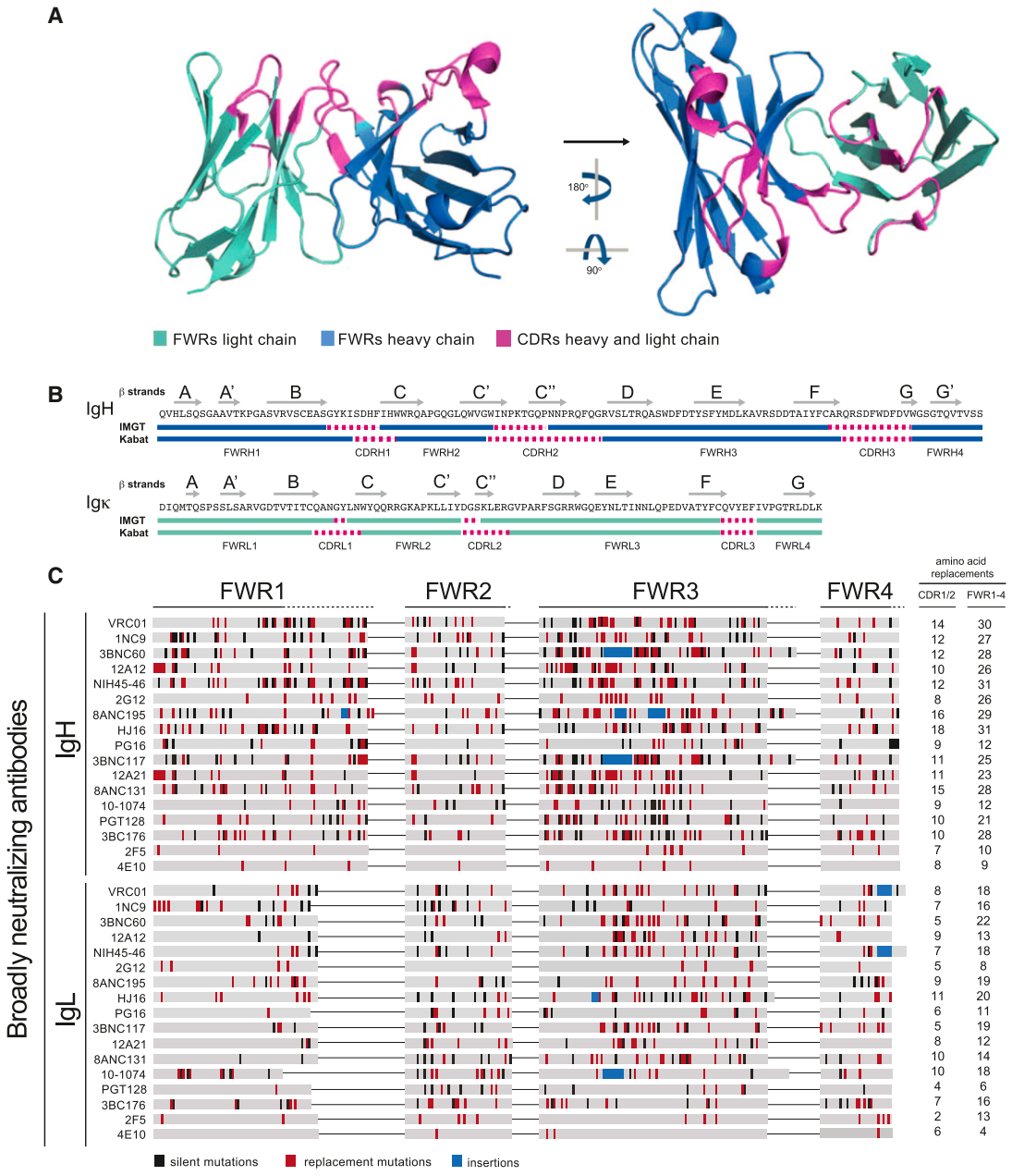

Figure 1. Somatic Mutations in the Framework Regions of HIV-1-Reactive Antibodies

(A) Ribbon representation of the variable domains of 3BNC60 (Scheid et al., 2011), illustrating the CDRs (magenta) and the FWRs of the immunoglobulin heavy (blue) and light (cyan) chain.

(B) Illustration of Kabat and IMGT CDR (magenta) and FWR (IgH, blue; IgL, cyan) assignments for the variable heavy and light chain domains of 3BNC60. Gray arrows indicate β strands defined by the crystal structure of the 3BNC60 Fab (Scheid et al., 2011).

(C) Position of FWR mutations in heavy and light chain of the 17 investigated antibodies with broad neutralizing activity (see also Data S1). Indicated are silent (black) and replacement (red) mutations. Insertions are illustrated in blue. For mAbs 2G12, 2F5, and 4E10, only amino acid replacements are shown (red). Number of replacement mutations within CDR1/2 and FWR1-4 are listed in the two columns at the very right (see also Table S1). HIV-1-reactive antibodies with limited neutralization are displayed in Figure S1.

Potent Broadly Neutralizing Antibodies

In contrast, reversion of the FWR mutations in most of the 17 broadly neutralizing antibodies decreased their binding to $gp140^{YU2}$ (Figures 2 and 3). Three of the antibodies, PG16 (Walker et al., 2009), 8ANC195 (Scheid et al., 2011), and 3BC176 (Klein et al., 2012a) bound poorly to $gp140^{YU2}$ when measured up to 8 μg/ml and differences in binding between mutated and reverted antibodies could not be evaluated (Figure 2).

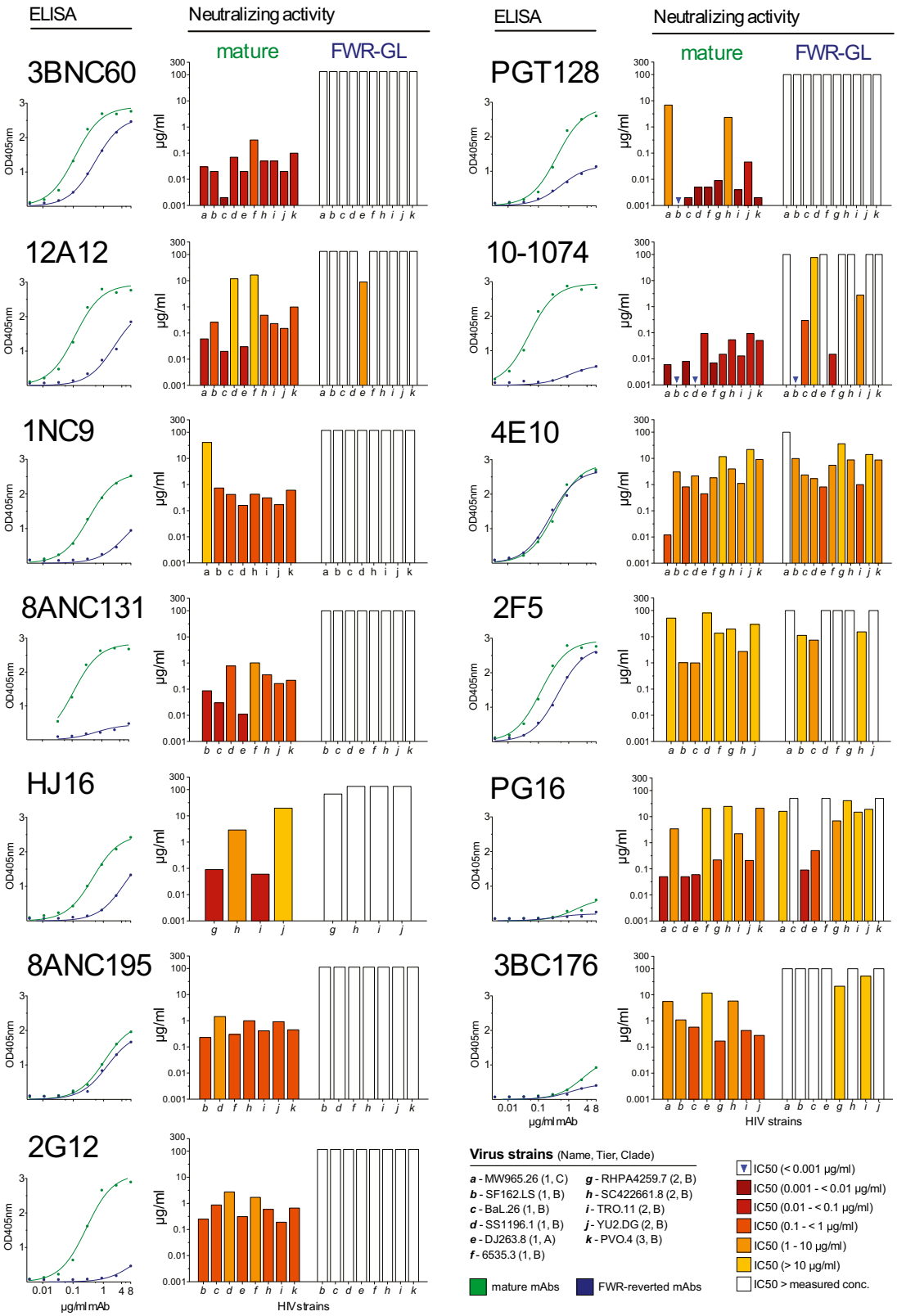

(legend on next page)

The neutralizing activity of the reverted antibodies was tested on a panel of 11 viruses (Tier 1 to Tier 3) representing HIV-1 clades A, B, and C (Figures 2 and 3 and Table S2). The majority of the FWR-GL antibodies lost nearly all their neutralizing activity against the tested strains. Similar results were also obtained when we produced FWR-GL antibody versions of VRC01, 3BNC60, and 8ANC131 according to IMGT alignment (Data S1F and Figure S2C). 4E10, which is among the least potent antibodies of the bNAbs tested, was the exception to the rule in retaining binding to $gp140^{YU2}$ as well as potency and breadth. PG16 retained most of its neutralizing breadth, but like the other bANbs, it lost potency by at least 10-fold after FWR reversion (geometric mean IC_{50} values increased from 0.95 to 9.69, Figure 2 and Table S2). 2G12 represents a special case for interpreting the effects of FWR residue reversion because the two Fabs of 2G12 IgG form a domain-swapped $(Fab)_2$ unit that creates a single antigen-binding site for recognizing a constellation of host-derived high mannose carbohydrates on gp120 (Calarese et al., 2003) (Figure S3). FWR residues are critical for the Fab dimerization via domain swapping (Huber et al., 2010) as well as for formation of a novel carbohydrate-binding site at the V_H-V_H' interface (Calarese et al., 2003).

To provide a general understanding of the relationship between direct FWR contacts and CDRH3 length on the degree of FWR somatic mutation, we analyzed these parameters for bNAbs for which antibody-antigen structures have been determined. No correlation was observed with CDRH3 length and degree of heavy chain, light chain, or total amount of FWR somatic mutation (Figure S4). Notably, however, the FWR contact surface area with antigen did correlate with the total number of amino acid changes in FWRs (Figure S4; p value = 0.0088; rho = 0.533).

To determine whether the effects of FWR reversion on binding and neutralization were simply due to alterations in contact residues, we selectively reverted all mutated FWR residues except for the contact residues ($FWR\text{-}GL^{CR+}$; Figure 3) in four bNAbs whose contact residues were known (VRC01, NIH45-46, 12A21, and 3BNC117) (Scheid et al., 2011; Wu et al., 2011; Zhou et al., 2010; unpublished data). Despite retaining their FWR contact residues, all of the partially reverted antibodies showed lower levels of binding by ELISA and SPR. Interestingly, the SPR-binding curves showed that loss of affinity appeared to be primarily due to an increased dissociation rate (off rate; k_d) (Figure 3). We conclude that FWR mutations enhance the affinity of broadly neutralizing antibodies primarily by decreasing the dissociation rate. Most importantly, $FWR\text{-}GL^{CR+}$ antibodies that retained somatically mutated FWR contact residues lost both neutralizing breadth and potency (Figure 3 and Table S2). We conclude that FWR mutations in noncontact residues are essential for the binding, breadth, and potency of most broadly neutralizing anti-HIV-1 antibodies.

Importance of a FWR Insertion in 3BNC60

Insertions and deletions are infrequent byproducts of somatic hypermutation that occur as a result of double-strand DNA breaks induced by deamination of neighboring cytidine residues by activation-induced cytidine deaminase (AID) (Pavri and Nussenzweig, 2011; Wilson et al., 1998). Nevertheless, several potent anti-CD4bs antibodies, including 3BNC60, contain insertions within FWRs that are acquired during somatic mutation (Scheid et al., 2011). Sequence analysis of the clonal relatives of 3BNC60 (clone RU01) revealed a correlation between the presence of this insertion and neutralizing activity (Figure 4). Superimposition of the 3BNC60 Fab structure onto the Fab portion of the NIH45-46/gp120 complex structure (Diskin et al., 2011) suggested that this insertion might enhance binding by interacting with the V1/V2 loop region that was truncated in the gp120 construct that was crystallized (Figure 5A) (similar results were found when superimposing the 3BNC60 Fab onto the 3BNC117 Fab, two nearly identical antibodies, in the 3BNC117/gp120 cocrystal structure [unpublished data]). To assess the effects of the insertion within FWR3 of the 3BNC60 heavy chain, we constructed a 3BNC60 mutant (3BNC60ΔI) in which the Trp-Asp-Phe-Asp insertion was removed (Figure 5B) and evaluated its neutralization activity against a panel of seven viruses chosen to include strains that were resistant to VRC01 but sensitive to 3BNC60 (Figure 5C). 3BNC60ΔI lost neutralization potency against all seven viruses. Adding the insertion to 3BNC55, a weaker variant of 3BNC60 isolated from the same donor (Scheid et al., 2011), increased the neutralization potency of 3BNC55+I compared to 3BNC55 against one viral strain (TRO.11) (Figure 5C). Addition of the insertion did not, however, restore the ability of a VRC01 plus insertion mutant to neutralize VRC01-resistant viruses (Data S1E and Table S2). Taken together, these results demonstrate that the FWR insertion is critical for the neutralization activity of 3BNC60, but that its ability to improve potency requires a precise recognition geometry that is not always found in other potent anti-CD4bs antibodies.

Crystal Structure of a Partially Reverted Fab

We previously noted a disruption in the canonical variable domain fold of the V_H domain of 3BNC60 (Scheid et al., 2011); namely, the main chain hydrogen bonding pattern between strands C'' and C' was disrupted by the presence of Pro61 (Kabat numbering position 60; IMGT position 68) located at the

Figure 2. Binding and Neutralization Activity of Mature and FWR-Reverted (FWR-GL) Broadly Neutralizing Antibodies

Evaluation of binding to $gp140^{YU2}$ ELISA (left) of mature antibodies (green) and antibodies with FWRs reverted to germline (FWR-GL; blue, Data S1B). Panels on the right compare IC_{50} values for neutralization of Tier 1 (MW965.26, SF162.LS, Bal.26, SS1196.1, DJ263.8, and 6535.3) Tier 2 (RHPA4259.7, SC422661.8, TRO.11, and YU2.DG), and Tier 3 (PVO.4) viruses (Table S2). Only viruses are shown that were neutralized by the mature version of the antibody. Neutralization activity is color coded (blue arrow, <0.001 μg/ml; dark red, IC_{50} between 0.001 and <0.01 μg/ml; red, 0.01–<0.1 μg/ml; orange, 0.1–<1 μg/ml; light orange, 1–10 μg/ml; yellow, >10 μg/ml; white, IC_{50} was not achieved up to the tested concentration). Antibodies (NIH45-46 and 3BN60) with reverted CDR1/2 are shown in Figure S2A and HIV-1-reactive antibodies with limited neutralization are displayed in Figure S2B. The FWRs of VRC01, 3BNC60, and 3BNC131 were also reverted according to IMGT (Giudicelli et al., 2006) and results are shown in Figure S2C. A detailed illustration of the FWR mutations in 2G12 is shown in Figure S3.

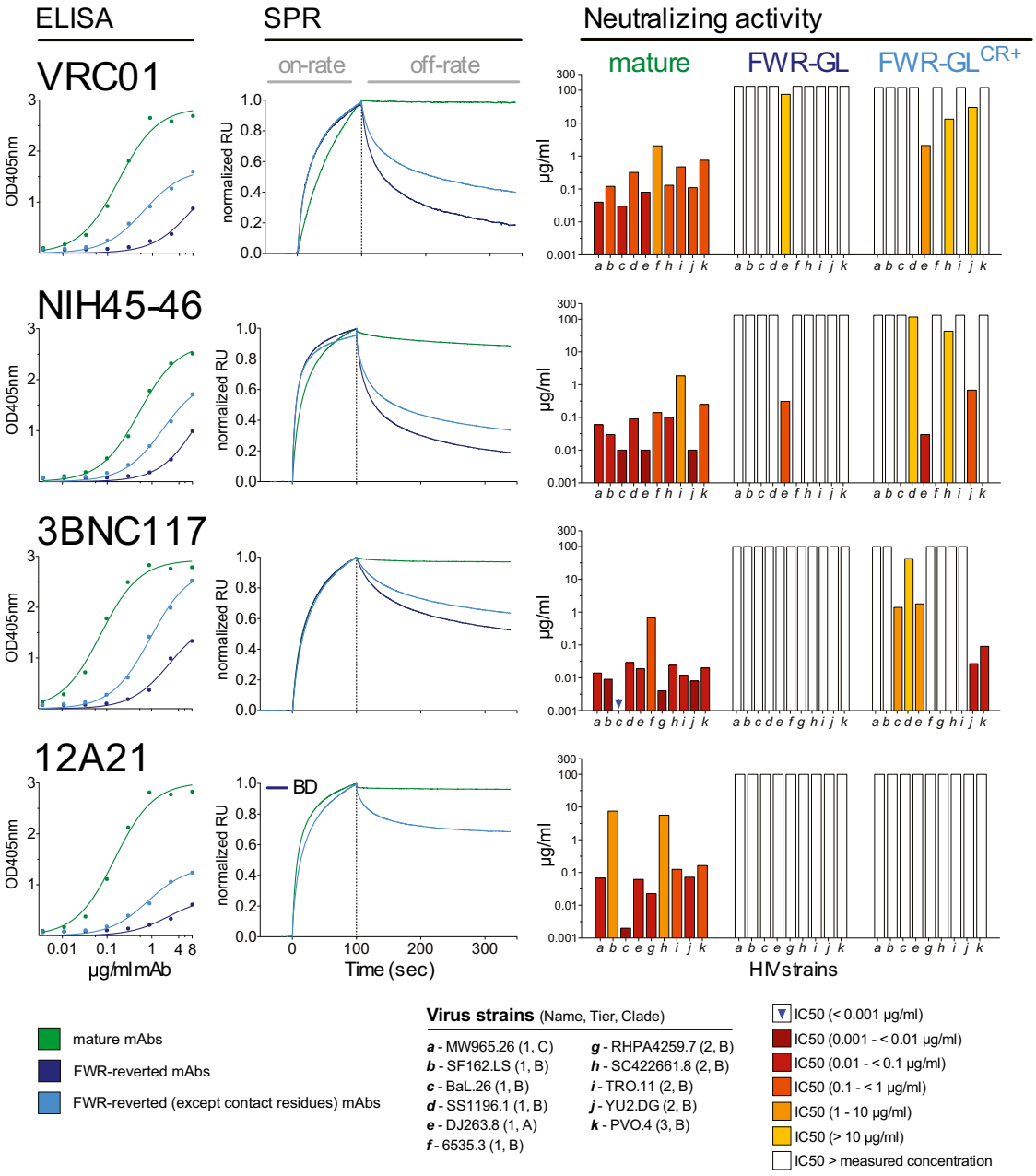

Figure 3. Binding and Neutralization Activity of Mature, FWR-GL, and FWR-GL^{CR+} Broadly Neutralizing Antibodies

Evaluation of binding to gp140^{YU2} ELISA (left) and SPR (middle) of mature antibodies (green), antibodies with FWRs reverted to germline (FWR-GL, blue), and antibodies with germline-reverted FWRs except gp120-contacting residues (FWR-GL^{CR+}; light blue; Data S1D). SPR results are shown for starting concentrations of 1 μM. BD (below detection; no binding of the antibody was observed). Panels on the right compare IC_{50} values for neutralization of Tier 1 to Tier 3 viruses (Table S2) as in Figure 2. Neutralization activity is color coded as indicated.

C-terminal end of strand C'' (Figure 6A). In contrast, the germline V_H sequence and other potent anti-CD4bs antibodies contain an alanine at this position (Scheid et al., 2011) (Data S1C and S1D). A proline within a β strand cannot form a main chain hydrogen bond with a carbonyl oxygen in an adjacent β strand because it lacks a hydrogen atom attached to its mainchain nitrogen (Figure 6A). Nevertheless, this proline mutation is associated with increased antibody potency among clonal members of the 3BNC60 family (Figure 4) (Scheid et al., 2011).

Although classified by Kabat (Kabat et al., 1991) as part of CDRH2, residue 61 is within the C'' β strand of the Ig V domain fold and is classified as a FWR residue by IMGT (Lefranc et al., 1999) (Figure 1B, S5). Thus we were interested in its potential role in antigen recognition. In the structure of the free 3BNC60

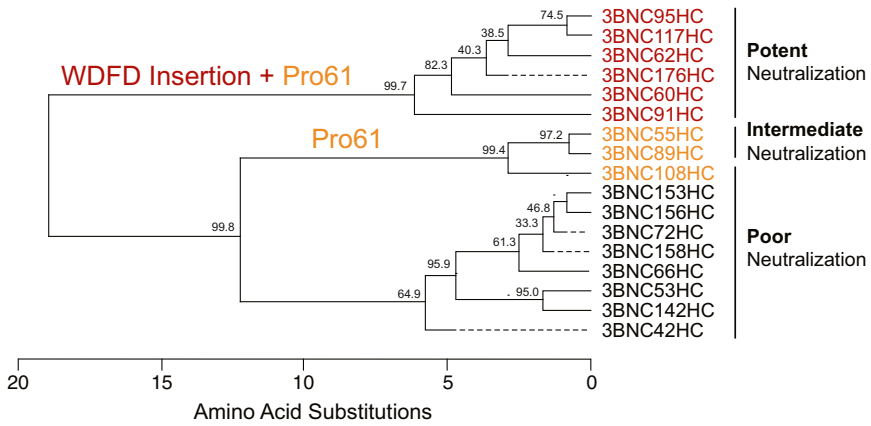

Figure 4. Effects of a FWR Insertion and a C'' β Strand Proline in Clone RU01

Phylogenetic tree of the antibodies (Ig heavy chain) derived from the RU01 clone that members include 3BNC117 and 3BNC60 (Scheid et al., 2011). Antibodies that carry both the four amino acid insertion in FWR3 and the A61P somatic mutation are shown in red, antibodies with only the A61P mutation are shown in orange, and antibodies without either feature are shown in black. Bootstrap values (1,000 trials, seed = 111) of the phylogenetic tree are indicated. Structure of 3BNC117 IGVH in its gp120-bound conformation is shown in Figure S5.

Fab, the region surrounding Pro61 is stabilized by a crystal contact (Figure S6) into a position that would clash with the CD4-binding loop of gp120 (Diskin et al., 2011; Scheid et al., 2011; Wu et al., 2011; Zhou et al., 2010). The potential clash with gp120 suggests that the region surrounding 3BNC60 Pro61 rearranges upon gp120 binding. Indeed, in the structure of a gp120 complex with the nearly identical antibody 3BNC117, the Fab exhibits a canonical V_H domain structure in its gp120-bound conformation (unpublished data) (Figure 6A). In addition, a murine Fab structure including a proline at this position shows minimal disruption of the β sheet including strand C'' (Stanfield et al., 1990) (Figure 6A).

To address the unusual properties of the C'' strand in 3BNC60, we solved the 2.65 Å crystal structure of 3BNC60^{P61A} (pdb code 4GW4), a single amino acid revertant mutant form of 3BNC60 (Figure 6A and Table S3). Like other Fabs containing alanine at position 61, including VRC01 (Zhou et al., 2010), VRC03, VRC-PG04 (Wu et al., 2011) and NIH45-46 (Diskin et al., 2011; Scheid et al., 2011), strand C'' of 3BNC60^{P61A} Fab exhibited normal hydrogen bonding to the neighboring C' strand (Figure 6A). Although the displaced region of strand C'' in the 3BNC60 Fab was involved in interactions with a crystallographic neighbor, perhaps stabilizing it in the conformation observed in the structure (Scheid et al., 2011), the corresponding region of strand C'' in the 3BNC60^{P61A} Fab did not contact a crystallographic neighbor despite isomorphous packing interactions in the 3BNC60 and 3BNC60^{P61A} crystals (Figure S6).

To further evaluate the effects of the Pro to Ala substitution in strand C,'' we compared the thermal stability of the 3BNC60 and 3BNC60^{P61A} Fabs (Figure 6B). Both proteins exhibited denaturation profiles characteristic of two-state (native to denatured) unfolding; however, the 3BNC60^{P61A} Fab showed increased thermal stability compared with the wild-type 3BNC60 Fab, as demonstrated by a higher transition midpoint (T_m) (Figure 6B).

The functional consequences of the Pro to Ala substitution were evaluated by comparing the neutralization potencies of 3BNC60 and 3BNC60^{P61A} IgGs against 19 representative strains sensitive to 3BNC60 (Figure 6C). The substitution affected the neutralizing activity of the antibody against seven of the strains (highlighted red; Figure 6C). We conclude that somatic mutation in the β sheet framework involving strand C'' is essential for the potency and breadth of 3BN60.

DISCUSSION

The β sandwich structure of the immunoglobulin fold lends itself to a natural division into relatively structurally invariant β strand FWRs and the more structurally diverse loops connecting the β strands, three of which form the hypervariable CDRs (Figures 1A and 1B). Thus, mutations in FWRs are usually poorly tolerated and selected against, whereas mutations in the structurally diverse CDRs are well tolerated. Starting with the first crystal structure of a Fab bound to a protein antigen (Amit et al., 1986), antibody-antigen complex structures have confirmed that residues within the CDR loops usually form the majority of contacts with the antigen. Therefore the primary role of FWR residues is to provide a scaffold for the antigen-contacting CDRs, as evidenced by the common practice of CDR grafting (Jones et al., 1986). However, we find that in contrast to most antibodies, including HIV-1-reactive antibodies with limited neutralizing activity (Figures S1 and S2B), somatically mutated FWR residues are critical for the breadth and potency of broadly neutralizing anti-HIV-1 antibodies (Figure 2 are 3). Thus, the FWRs in these unusual antibodies serve an essential function beyond that of a scaffold for antigen-binding CDRs.

Understanding the excessive somatic hypermutation found in bNAbs requires consideration of the process by which antibodies are mutated. B cells undergo somatic hypermutation in germinal centers during T-cell-dependent immune responses (Victora and Nussenzweig, 2012). The mutations are introduced by AID, which preferentially targets cytosines embedded in RGYW nucleotide sequences (in which R can be A or G, Y can be C or T, and W can be A or T) in antibody variable regions (Pavri and Nussenzweig, 2011). However, mutations are not limited to cytidine residues because error prone repair mechanisms also contribute to the repair of the initial lesions (Pavri and Nussenzweig, 2011; Peled et al., 2008). Thus, the mutation process is far more random than would occur if only RGYW cytidines were targeted.

Mutations that enhance antibody affinity are rare, but they are positively selected in the germinal center as a result of increased antigen uptake and MHC-peptide presentation, which results in increased T-cell-mediated help (Victora and Nussenzweig, 2012). Mutations that increase antibody affinity can do so by increasing the on-rate or by decreasing the off rate. The on-rate

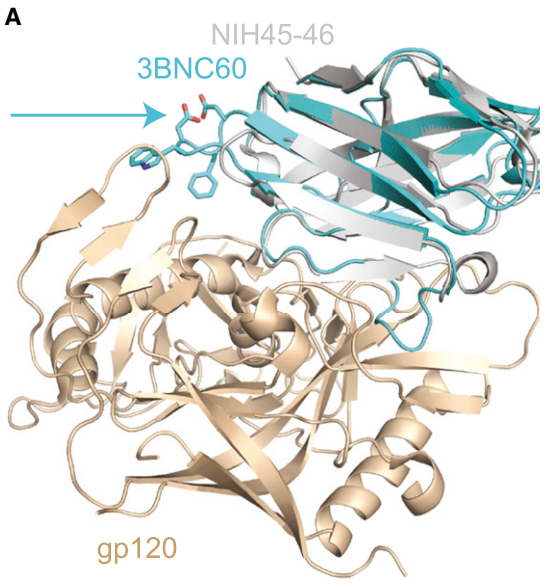

B

	FWRH3
3BNC60	RVSLTRQASWDFDTYSFYMDLKAVRSDDTAIYFCAR
3BNC60ΔI	RVSLTRDTF----DEMLYMDLKAVRSDDTAIYFCAR
3BNC55	RLTLTRDTF----DEMLYMDLRGLRSDDTGIYFCAR
3BNC55+I	RLTLTRQASWDFDTYSFYMDLRGLRSDDTGIYFCAR

C

Virus	Clade	3BNC60	3BNC60ΔI
T211	CRF02_AG	0.37	47.4
CAP210.2.00.E8	C	6.6	>50
3817.v2.c59	CD	0.15	46.3
62357_14_D3_4589	B (T/F)	0.05	19.6
Q259.d2.17	A	0.02	>50
3016.v5.c45	D	1.58	>50
Du172.17	C	1.41	>50

		3BNC55	3BNC55+I
BaL.26	B	>50	>50
TRO.11	B	18.4	0.93
T250	CRF02_AG	0.24	0.11
3016.v5.c45	D	>50	50

Figure 5. Analysis of 3BNC60 Insertion

(A) Superimposition of the structure of the V_H domain of 3BNC60 (cyan) (Scheid et al., 2011) onto the NIH45-46 V_H domain from cocrystal structure of NIH45-46 (gray) bound to gp120 (gold) (Diskin et al., 2011) highlighting the four residue insertion in FWR3 of 3BNC60 (cyan arrow) and a potential interaction between the insertion and the gp120 V1/V2 loop (note that the V1/V2 loop was truncated in the gp120 construct used for cocrystallization with NIH45-46 and VRC01) (Diskin et al., 2011; Zhou et al., 2010).

(B) Alignment of the heavy chain FWR3 sequences of 3BNC60 (Scheid et al., 2011), 3BNC60 without the 3BNC60 insertion (3BNC60ΔI), 3BNC55 (Scheid et al., 2011), and 3BNC55 containing the 3BNC60 insertion (3BNC55+I; Data S1E). The four amino acid insertion in FWR3 of 3BNC60 is shown in cyan and the region grafted into 3BNC60 from 3BNC55 in order to delete the insertion without disrupting the structure is shown in gray. The amino acid changes to introduce the insertion into 3BNC55 are shown in blue.

(C) In vitro neutralization data (IC_{50} values in μg/ml) comparing the potencies of the antibodies. The upper panel compares neutralization of selected viral strains by 3BNC60 and 3BNC60ΔI. The lower panel compares the neutralization by a less potent member of the RU01 clone (3BNC55), in which the FWR3 insertion of 3BNC60 was introduced (3BNC55+I). Reduced and increased neutralization activity of the engineered antibodies (3BNC60ΔI, 3BNC55+I) is highlighted red and green, respectively. Neutralization data on VRC01 with and without the 3BNC60 insertion is displayed in Table S2.

is diffusion limited, and the off rate is limited by speed of antigen internalization because once the antigen is in a degradative endosome it will be digested irrespective of its rate of release from the antibody (Batista and Neuberger, 1998; Foote and Milstein, 1991). Thus, naturally developing antibody affinities do not normally exceed an affinity of 10^{-11} M. In humans, this degree of affinity maturation is usually achieved with an average of 10–15 nucleotide mutations focused in the antigen contact residues in the CDR loops.

Although somatic mutations occur throughout the variable region, mutations that alter the amino acid coding sequence of the antibody accumulate preferentially in CDRs in part because of higher level of degeneracy of the codons used in the FWRs (Jolly et al., 1996; Reynaud et al., 1995; Wagner et al., 1995). Any alterations in the FWRs are constrained by the fact that they must conserve the overall structure of the antibody because B cells that fail to express surface Ig are destined to die by apoptosis (Rajewsky, 1996). Indeed the FWRs appear to have evolved a nucleotide coding sequence that resists mutation in order to prevent changes in relatively invariant β strands that are required to scaffold the CDR loops (Jolly et al., 1996; Reynaud et al., 1995; Wagner et al., 1995). Thus, a large number of random nucleotide mutations would be required to alter the FWRs in a manner that optimizes the broadly neutralizing anti-HIV-1 antibodies while conserving essential structural elements.

The mutated FWR residues in the broadly neutralizing anti-HIV-1 antibodies contribute to binding and enhance breadth and potency in several different ways. In some cases, the substituted FWR residues directly contact the antigen; for example, crystal structures of the bNAbs VRC01 and NIH45-46 complexed with gp120 (Diskin et al., 2011; Zhou et al., 2010) reveal that FWR residue Arg71 in both VRC01 and NIH45-46 forms a salt bridge with gp120 residue Asp368. Thus, FWR mutation can serve to directly increase the binding interface by recruiting portions of the antibody that are not normally involved in antigen recognition. Moreover the ligand-bound structure of PGT128 (Pejchal et al., 2011) shows that the carbohydrate attached to $Asn121_{gp120}$ interacts with residues within the C" β strand of the antibody heavy chain (Trp56, Thr57, His59 and Lys64). Two of these residues represent somatic mutations. In other cases, FWR residues do not appear to directly contact the antigen, yet are required for potency. For example, the FWRs of PG16 do not contribute substantially to direct antigen contacts and interaction with the antigen is mainly mediated through a long CDR3 loop (unpublished data) (Figure S4).

Somatic mutation of residues within the β sheet framework of the V domain can also indirectly affect the V domain structure so

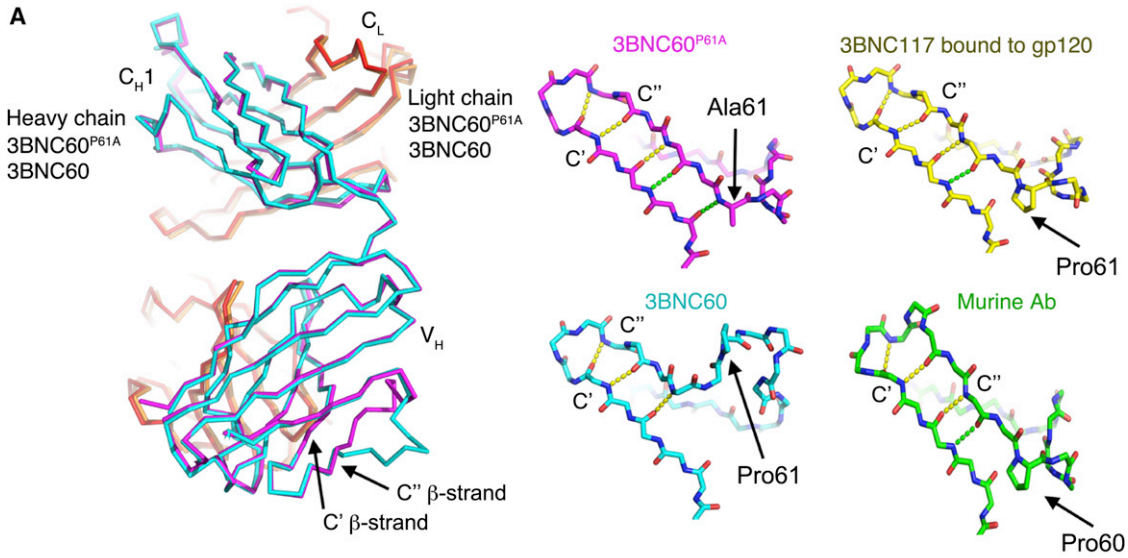

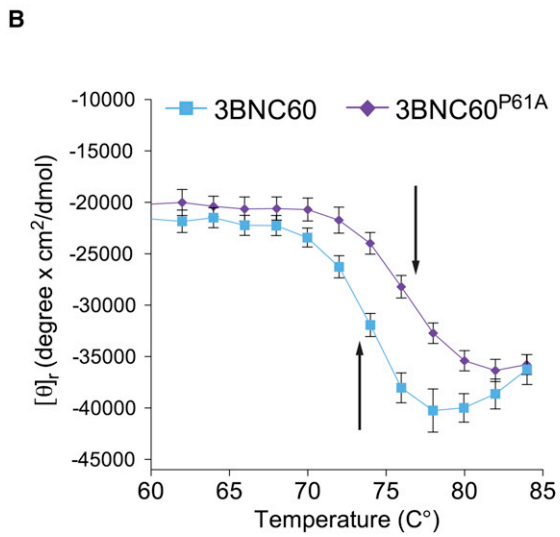

C Neutralization IC_{50} (μg/ml)

Virus	Clade	3BNC60	3BNC60^{P61A}
6535.3	B	**0.66**	**>50**
CAP210.2.00.E8	C	**4.83**	**34.31**
6480.v4.c25	CD	0.02	0.02
6952.v1.c20	CD	**0.14**	**1.03**
CNE52	BC	0.02	0.04
3365.v2.c2	A	0.01	0.01
R2184.c04	CRF01_AE	0.03	0.02
C3347.c11	CRF01_AE	0.04	0.04
X1254_c3	G	**0.07**	**1.24**
A07412M1.vrc12	D	0.05	0.04
6811.v7.c18	CD	0.09	0.09
Ce1086_B2	C (T/F)	0.1	0.12
249M B10	C (T/F)	0.09	0.07
R3265_c6	CRF01_AE	**1.63**	**>50**
QH0692	B	0.57	0.63
Cap45	C	**2.1**	**>50**
T257-31	B	0.34	0.26
TRO.11	B	0.04	0.06
Du172.17	C	**1.15**	**40.16**

Figure 6. Comparison of 3BNC60 and 3BNC60^{P61A} Structures, Thermal Denaturation Profiles, and Neutralizing Activities

(A) Left: 3BNC60^{P61A} (Table S3; magenta, heavy chain; orange, light chain) was superimposed on the structure of 3BNC60 (cyan, heavy chain; red, light chain). The C'' β strand within FWR3 of the V_H domain differs in conformation between the two structures. Middle/right: Close-up of the C' and C'' β strands of 3BNC60^{P61A} (magenta), 3BNC117 bound to go120 (yellow), 3BNC60 (cyan), and a murine Fab (green). The main chain atoms of the V_H domain C' and C'' β strands of 3BNC60^{P61A} exhibit a typical hydrogen-bonding pattern for an antiparallel β sheet. Three of the five inter-β strand hydrogen bonds in 3BNC60^{P61A} are found in all three structures (yellow dashed lines), whereas 3BNC60 lacks two and the murine Fab/3BNC117 lacks one of the hydrogen bonds (green dashed lines in 3BNC60^{P61A}). Cocrystallization of the 3BNC60-relative 3BNC117 with gp120 shows that Proline61 is accommodated without disrupting the C'-C'' β sheet when 3BNC117 is bound to gp120. Overview of the packing in crystals of 3BNC60 and 3BNC60^{P61A} is shown in Figure S6.

(B) Thermal denaturation profiles of the 3BNC60 and 3BNC60^{P61A} Fabs monitored by the CD signal at 218 nm. T_ms (indicated with arrows) were derived by estimating the half-point of the ellipticity change between the beginning and end of each transition. Errors bars indicate SD.

(C) In vitro neutralization data (IC_{50} values in μg/ml) comparing the 3BNC60 and 3BNC60^{P61A} IgGs for a panel of 19 viruses. Reduced neutralization activity is highlighted in red. An additional nine viral strains (T250-4, T278-50, 620345.c01, X2088_c9, 89-F1_2_25, 6540.v4.c1, CAP45.2.00.G3, 6545.v4.c1, and Du422.1) were resistant to both 3BNC60 and 3BNC60^{P61A}. The 3BNC60^{P61A} mutant was not significantly more potent than 3BNC60 against any of the 28 strains tested.

as to facilitate HIV-1 antigen recognition, as exemplified by the Pro61 residue in the broadly neutralizing antibodies 3BNC60/3BNC117 (Figure 6). Residue 61 falls within the β sheet framework of the Ig V domain. Substitution of this proline to the germline alanine in 3BNC60 resulted in increased thermal stability, but a loss of neutralization activity against some HIV-1 strains. The structural effects of the proline to alanine substitution were revealed by comparison of the crystal structures of the 3BNC60^{P61A} and 3BNC60 Fabs: the V_H domain β strand that was disrupted by the proline in the 3BNC60 structure was

restored to its canonical position in the mutant Fab structure (Figure 6A). In the 3BNC117/gp120 structure (unpublished data), the Pro61-containing β strand is shifted from its position in the free 3BNC60 structure (where it was likely stabilized into the observed conformation by crystal packing forces) in order to avoid clashing with the CD4-binding loop in gp120, as predicted previously for 3BNC60/gp120 complexes (Scheid et al., 2011) (Figure 6A). The lower thermal stability of 3BNC60 Fab compared with 3BNC60^{P61A} Fab (Figure 6B) is consistent with flexibility that would allow this sort of displacement.

Superimposition of the 3BNC60^{P61A} Fab into the 3BNC117/gp120 cocrystal structure (unpublished data) suggests that an alanine would be accommodated equally as well as a proline at position 61, and the fact that the P61A mutant of 3BNC60 neutralizes some HIV-1 strains equally as well as wild-type 3BNC60 suggests that Pro61 does not make any direct contacts to HIV-1 gp120 that are critical for binding to gp120 and neutralization. Instead we speculate that in the case of 3BNC60 and 3BNC117, the ability to disrupt the C'–C'' portion of the C''C'CFG β sheet, which provides flexibility for V_H residues 60–66, is necessary in order to accommodate antigenic sequence heterogeneity in or near the gp120 V5 loop. Taken together, these results provide a counterintuitive example of a neutral or functionally favorable somatic mutation that decreases the Fab stability by disrupting the canonical V_H domain fold, allowing flexibility of the β sheet framework that is needed for optimal antigen binding and neutralization (Figure 6C).

The high level of mutation found in broadly neutralizing antibodies would be difficult to explain in the context of an immune response to a conventional antigen and a single round of germinal center selection. However, HIV-1 differs from conventional antigens in that it presents the host with a continuously evolving target that is selected on the basis of its ability to evade the antibody response (Wei et al., 2003). We speculate that HIV-1 variants selected for their ability to evade antibodies due to lowered affinity will recall memory B cells to the germinal center for additional rounds of mutation and selection. Thus, iterative rounds of antibody mutation, selection, and viral escape would facilitate the accumulation of essential mutations in the FWR that conserve some key aspects of antibody structure while altering others to enhance anti-HIV-1 breadth and potency.

In conclusion, our experiments suggest a molecular and a structural rationale for the requirement of high levels of somatic mutation found in broadly neutralizing antibodies and possibly for the observation that it takes several years for infected individuals to develop such antibodies. The high relevance of FWR mutations should be considered in the approach to designing an HIV-1 vaccine.

EXPERIMENTAL PROCEDURES

Sequence Analysis of HIV-1-Reactive Antibodies

Analysis of heavy and light chain gene segment usage, number of somatic mutations, and the presence of deletions or insertions was carried out using the NCBI IgBLAST software (http://www.ncbi.nlm.nih.gov/igblast/). CDRs and FWRs were designated according to the Kabat (Wu and Kabat, 1970) (Figures 1, Data S1A–S1E, and Table S1) or IMGT numbering system (Figure 1B and Data S1F) using IgBLAST software. VRC01- and NIH45-46-FWR-GL^{CR+} antibodies were designed to carry reverted FWRs with unreverted contact residues based on the crystal structure of a gp120-VRC01 complex (Zhou et al., 2010). 3BNC117- and 12A21-FWR-GL^{CR+}-antibodies were based on the cocrystal structures as described by Peter Kwong and colleagues (PDB codes 4JPV and 4JPW, unpublished data). Any residue with a buried surface area (BSA) greater than 5 Å^2 was considered significant.

Sequences of the RU01 clone (Scheid et al., 2011) were aligned using Clustal V from the DNAstar package using PAM 250 matrix. The phylogenetic tree was constructed using the DNAstar package, which employs a neighbor joining method. Bootstrap values (1,000 trials, seed = 111) are as indicated (Figure 4). Classification of neutralization potency (RU01 clone) was based on the neutralization activity. Antibodies were grouped into potent, intermediate, and poor neutralizers by taking into account the potency (IC_{50}) against BaL.26, DJ263.8, 6535.3, RHPA4259.7, Tro.11, PVO.4, and YU2.DG as well as breadth (number of the tested strains neutralized) (Scheid et al., 2011).

Cloning, Expression, and Purification of Immunoglobulins

The variable regions of all mature, FWR-GL, FWR-GL^{CR+}, and CDR1/2-GL antibodies were cloned into the same IgH, Igκ, or Igλ backbones encoding the constant domains of the antibodies. Reversions of the FWRs were introduced by overlapping PCR or by DNA synthesis (Integrated DNA Technologies). The sequence of 17b was obtained from the structure with CD4 (pdb code 1G9M). The P61A mutation was introduced into the 3BNC60 heavy chain gene by site-directed mutagenesis using QuikChange Site-Directed Mutagenesis Kit (Agilent Technologies). Because the region of the FWR3 insertion is highly mutated and the exact location of inserted amino acids is difficult to determine, surrounding regions from 3BNC55 and 3BNC60 were included in each construct (Figure 5B). Likewise, the residues surrounding the engrafted insertion in VRC01 were chosen based on the crystal structures of VRC01 and 3BNC60 (Data S1E) (Scheid et al., 2011; Zhou et al., 2010). Antibodies were expressed and purified as previously described (Mouquet et al., 2011) (Diskin et al., 2011).

ELISA

ELISAs for analyzing antibody binding to gp140^{YU2} (Figures 2, 3, and S2) was performed as previously described (Mouquet et al., 2011).

Neutralization Assays

Neutralizing activities of mature, FWR-GL, FWR-GL^{CR+}, and CDR1/2-GL antibodies were determined using a TZM.bl assay as previously described (Diskin et al., 2011; Li et al., 2005; Montefiori, 2005; Seaman et al., 2010). Briefly, TZM.bl cells were infected with different Tier 1 to Tier 3 HIV-1-Env-pseudoviruses in the presence of serial dilutions of the antibodies tested. Antibodies with neutralizing activity inhibit the infection and a reduction of luciferase reporter gene expression can be measured 48 hr after infection. IC_{50} values were calculated based on the antibody concentration that resulted in a 50% reduction of relative luminescence units (RLU).

Surface Plasmon Resonance

Experiments were performed with a Biacore T200 (Biacore) as described previously (Diskin et al., 2011). Briefly, YU-2 gp140 was primary amine-coupled on CM5 chips (Biacore) at an immobilization level of 1,000 RUs. IgG antibodies were injected over flow cells at 1 μM, at flow rates of 90 μl/min. The sensor surface was regenerated by a 50 s injection of 10 mM glycine-HCl pH 2.5 at a flow rate of 90 μl/min.

Crystallization and Structure of 3BNC60^{P61A} Fab

3BNC60^{P61A} Fab (pdb code 4GW4) was concentrated to 13.7 mg/ml in 20 mM Tris (pH 8.0), 150 mM sodium chloride, 0.02% sodium azide (TBS) buffer. Crystals of Fab 3BNC60^{P61A} were obtained by mixing a protein solution at 13.7 mg/ml with 16% polyethylene glycol 6000, 0.1 M citric acid (pH 3.9), 0.15 M lithium sulfate monohydrate at 20°C. For cryoprotection, crystals were briefly soaked in mother liquor solutions supplemented with 15% and subsequently with 30% ethylene glycol before flash cooling in liquid nitrogen.

3BNC60^{P61A} Fab crystals grew in space group $P2_1$ (a = 64.6, b = 154.9, c = 74.2 Å; β = 109.7°) and were isomorphous to 3BNC60 Fab crystals (Scheid

et al., 2011). Data were indexed, integrated, and scaled using XDS (Kabsch, 2010). We used Phaser (McCoy et al., 2007) to find a molecular replacement solution for two Fabs per asymmetric unit (chains A and H and chains B and L for the heavy and light chains, respectively) using the 3BNC60 Fab structure (PDB code 3RPI) as a search model after omitting residues 59–66 of the heavy chain. Residues 59–66 were built into F_o-F_c difference electron density maps after a few rounds of iterative refinement including noncrystallographic symmetry restraints using Phenix (Adams et al., 2010) and Coot (Emsley et al., 2010). The final 2.65 Å resolution atomic model for two 3BNC60^{P61A} Fabs (R_{work} = 21.5%; R_{free} = 25.6%) includes 12,598 protein atoms (of which 6,198 are hydrogen atoms), 199 water molecules, and 28 ligand atoms (N-acetylglucosamine attached to Asn70 of the light chain) (Table S3). Using the numbering established for the 3BNC60 Fab structure (Scheid et al., 2011), the residues included in the final model are 1–132 and 141–217 of chain H, 2–132 and 141–217 of chain A, 4–198 of chain L, and 4–199 of chain B. The first glutamine of the 3BNC60^{P61A} heavy chain was modeled as 5-pyrrolidone-2-carboxylic acid. A total of 94.5%, 5.3%, and 0.3% of the residues were in the favored, allowed and disallowed regions of the Ramachandran plot, respectively.

Thermal Stability Comparisons

Purified 3BNC60 and 3BNC60^{P61A} Fabs were concentrated to 10 μM in 1 mM dithiothreitol and 5 mM sodium chloride for CD studies. Far UV wavelength scans (200 nm to 250 nm) were recorded in 1 nm increments using an averaging time of 5 s on an Aviv 62A DS spectropolarimeter. Both spectra showed a distinct negative signal at 218 nm, thus this wavelength was chosen for the thermal stability comparisons. Thermostability profiles were obtained by monitoring the CD signal at 218 nm as the temperature was raised from 40°C to 95°C in 2°C increments, allowing 1 min of equilibration time after each temperature step and averaging the CD signal over 30 s of measurement. Transition midpoints (T_ms) were obtained by estimating the half-point of the ellipticity change between the native and denatured states.

SUPPLEMENTAL INFORMATION

Supplemental Information includes Extended Experimental Procedures, six figures, three tables, and one data file, and can be found with this article online at http://dx.doi.org/10.1016/j.cell.2013.03.018.

ACKNOWLEDGMENTS

We thank Louise Scharf for her help on generating structural images and Kai-Hui Yao for technical assistance. We thank Paola Marchovecchio and Han Gan for preparation of 3BNC60^{P61A} as well as the members of the Nussenzweig and Bjorkman laboratory for helpful discussions. We also thank R. Wyatt for the YU2-gp140 plasmid; Davide Corti and Antonio Lanzavecchia for the HJ16 plasmids, and Francine McCutchan, Beatrice Hahn, David Montefiori, Michael Thomson, Ronald Swanstrom, Lynn Morris, Jerome Kim, Linqi Zhang, Dennis Ellenberger, and Carolyn Williamson for contributing HIV-1 envelope plasmids used in neutralization assays. F.K. was supported by the German Research Foundation (DFG, KL 2389/1-1), the Stavros Niarchos Foundation and the Robert Mapplethorpe Foundation. C.G. and R.-B.I. were supported by The German National Academic Foundation. I.G., M.P., T.Z., and P.D.K. were supported by intramural funding to the Vaccine Research Center, NIAID, NIH. M.S.S., P.J.B., and M.C.N. were supported by the Bill and Melinda Gates Foundation (M.S.S., Comprehensive Antibody Vaccine Immune Monitoring Consortium grant 1032144; P.J.B. and M.C.N., Collaboration for AIDS Vaccine Discovery grants 38660 [P.J.B.] and OPP1033115 [M.C.N.]). M.C.N is supported by the CHAVI-ID Award UM1AI100663 and The NIH grant AI081677. M.C.N. and P.J.B. are HHMI investigators.

Received: April 6, 2012
Revised: January 7, 2013
Accepted: March 11, 2013
Published: March 28, 2013

REFERENCES

Adams, P.D., Afonine, P.V., Bunkóczi, G., Chen, V.B., Davis, I.W., Echols, N., Headd, J.J., Hung, L.W., Kapral, G.J., Grosse-Kunstleve, R.W., et al. (2010). PHENIX: a comprehensive Python-based system for macromolecular structure solution. Acta Crystallogr. D Biol. Crystallogr. *66*, 213–221.

Amit, A.G., Mariuzza, R.A., Phillips, S.E., and Poljak, R.J. (1986). Three-dimensional structure of an antigen-antibody complex at 2.8 A resolution. Science *233*, 747–753.

Amzel, L.M., and Poljak, R.J. (1979). Three-dimensional structure of immunoglobulins. Annu. Rev. Biochem. *48*, 961–997.

Batista, F.D., and Neuberger, M.S. (1998). Affinity dependence of the B cell response to antigen: a threshold, a ceiling, and the importance of off-rate. Immunity *8*, 751–759.

Buchacher, A., Predl, R., Strutzenberger, K., Steinfellner, W., Trkola, A., Purtscher, M., Gruber, G., Tauer, C., Steindl, F., Jungbauer, A., et al. (1994). Generation of human monoclonal antibodies against HIV-1 proteins; electrofusion and Epstein-Barr virus transformation for peripheral blood lymphocyte immortalization. AIDS Res. Hum. Retroviruses *10*, 359–369.

Calarese, D.A., Scanlan, C.N., Zwick, M.B., Deechongkit, S., Mimura, Y., Kunert, R., Zhu, P., Wormald, M.R., Stanfield, R.L., Roux, K.H., et al. (2003). Antibody domain exchange is an immunological solution to carbohydrate cluster recognition. Science *300*, 2065–2071.

Corti, D., Langedijk, J.P., Hinz, A., Seaman, M.S., Vanzetta, F., Fernandez-Rodriguez, B.M., Silacci, C., Pinna, D., Jarrossay, D., Balla-Jhagjhoorsingh, S., et al. (2010). Analysis of memory B cell responses and isolation of novel monoclonal antibodies with neutralizing breadth from HIV-1-infected individuals. PLoS ONE *5*, e8805.

Diskin, R., Scheid, J.F., Marcovecchio, P.M., West, A.P., Jr., Klein, F., Gao, H., Gnanapragasam, P.N., Abadir, A., Seaman, M.S., Nussenzweig, M.C., and Bjorkman, P.J. (2011). Increasing the potency and breadth of an HIV antibody by using structure-based rational design. Science *334*, 1289–1293.

Doria-Rose, N.A., Klein, R.M., Daniels, M.G., O'Dell, S., Nason, M., Lapedes, A., Bhattacharya, T., Migueles, S.A., Wyatt, R.T., Korber, B.T., et al. (2010). Breadth of human immunodeficiency virus-specific neutralizing activity in sera: clustering analysis and association with clinical variables. J. Virol. *84*, 1631–1636.

Emsley, P., Lohkamp, B., Scott, W.G., and Cowtan, K. (2010). Features and development of Coot. Acta Crystallogr. D Biol. Crystallogr. *66*, 486–501.

Foote, J., and Milstein, C. (1991). Kinetic maturation of an immune response. Nature *352*, 530–532.

Giudicelli, V., Duroux, P., Ginestoux, C., Folch, G., Jabado-Michaloud, J., Chaume, D., and Lefranc, M.P. (2006). IMGT/LIGM-DB, the IMGT comprehensive database of immunoglobulin and T cell receptor nucleotide sequences. Nucleic Acids Res. *34*(Database issue), D781–D784.

Gorny, M.K., Xu, J.Y., Karwowska, S., Buchbinder, A., and Zolla-Pazner, S. (1993). Repertoire of neutralizing human monoclonal antibodies specific for the V3 domain of HIV-1 gp120. J. Immunol. *150*, 635–643.

Huang, J., Ofek, G., Laub, L., Louder, M.K., Doria-Rose, N.A., Longo, N.S., Imamichi, H., Bailer, R.T., Chakrabarti, B., Sharma, S.K., et al. (2012). Broad and potent neutralization of HIV-1 by a gp41-specific human antibody. Nature *491*, 406–412.

Huber, M., Le, K.M., Doores, K.J., Fulton, Z., Stanfield, R.L., Wilson, I.A., and Burton, D.R. (2010). Very few substitutions in a germ line antibody are required to initiate significant domain exchange. J. Virol. *84*, 10700–10707.

Jolly, C.J., Wagner, S.D., Rada, C., Klix, N., Milstein, C., and Neuberger, M.S. (1996). The targeting of somatic hypermutation. Semin. Immunol. *8*, 159–168.

Jones, P.T., Dear, P.H., Foote, J., Neuberger, M.S., and Winter, G. (1986). Replacing the complementarity-determining regions in a human antibody with those from a mouse. Nature *321*, 522–525.

Kabat, E., Wu, T.T., Reid-Miller, M., Perry, H.M., Gottesman, K.S., and Foeller, C. (1991). Sequences of Proteins of Immunological Interest (Bethesda, MD: US Department of Health and Human Services, National Institutes of Health).

Kabsch, W. (2010). Integration, scaling, space-group assignment and post-refinement. Acta Crystallogr. D Biol. Crystallogr. *66*, 133–144.

Klein, F., Gaebler, C., Mouquet, H., Sather, D.N., Lehmann, C., Scheid, J.F., Kraft, Z., Liu, Y., Pietzsch, J., Hurley, A., et al. (2012a). Broad neutralization by a combination of antibodies recognizing the CD4 binding site and a new conformational epitope on the HIV-1 envelope protein. J. Exp. Med. *209*, 1469–1479.

Klein, F., Halper-Stromberg, A., Horwitz, J.A., Gruell, H., Scheid, J.F., Bournazos, S., Mouquet, H., Spatz, L.A., Diskin, R., Abadir, A., et al. (2012b). HIV therapy by a combination of broadly neutralizing antibodies in humanized mice. Nature *492*, 118–122.

Lefranc, M.P., Giudicelli, V., Ginestoux, C., Bodmer, J., Müller, W., Bontrop, R., Lemaitre, M., Malik, A., Barbié, V., and Chaume, D. (1999). IMGT, the international ImMunoGeneTics database. Nucleic Acids Res. *27*, 209–212.

Li, M., Gao, F., Mascola, J.R., Stamatatos, L., Polonis, V.R., Koutsoukos, M., Voss, G., Goepfert, P., Gilbert, P., Greene, K.M., et al. (2005). Human immunodeficiency virus type 1 env clones from acute and early subtype B infections for standardized assessments of vaccine-elicited neutralizing antibodies. J. Virol. *79*, 10108–10125.

Mascola, J.R., Stiegler, G., VanCott, T.C., Katinger, H., Carpenter, C.B., Hanson, C.E., Beary, H., Hayes, D., Frankel, S.S., Birx, D.L., and Lewis, M.G. (2000). Protection of macaques against vaginal transmission of a pathogenic HIV-1/SIV chimeric virus by passive infusion of neutralizing antibodies. Nat. Med. *6*, 207–210.

McCoy, A.J., Grosse-Kunstleve, R.W., Adams, P.D., Winn, M.D., Storoni, L.C., and Read, R.J. (2007). Phaser crystallographic software. J. Appl. Cryst. *40*, 658–674.

Mikell, I., Sather, D.N., Kalams, S.A., Altfeld, M., Alter, G., and Stamatatos, L. (2011). Characteristics of the earliest cross-neutralizing antibody response to HIV-1. PLoS Pathog. *7*, e1001251.

Moldt, B., Rakasz, E.G., Schultz, N., Chan-Hui, P.Y., Swiderek, K., Weisgrau, K.L., Piaskowski, S.M., Bergman, Z., Watkins, D.I., Poignard, P., and Burton, D.R. (2012). Highly potent HIV-specific antibody neutralization in vitro translates into effective protection against mucosal SHIV challenge in vivo. Proc. Natl. Acad. Sci. USA *109*, 18921–18925.

Montefiori, D.C. (2005). Evaluating neutralizing antibodies against HIV, SIV, and SHIV in luciferase reporter gene assays. Curr. Protoc. Immunol., *Chapter 12*, Unit 12 11.

Morris, L., Chen, X., Alam, M., Tomaras, G., Zhang, R., Marshall, D.J., Chen, B., Parks, R., Foulger, A., Jaeger, F., et al. (2011). Isolation of a human anti-HIV gp41 membrane proximal region neutralizing antibody by antigen-specific single B cell sorting. PLoS ONE *6*, e23532.

Mouquet, H., Scheid, J.F., Zoller, M.J., Krogsgaard, M., Ott, R.G., Shukair, S., Artyomov, M.N., Pietzsch, J., Connors, M., Pereyra, F., et al. (2010). Polyreactivity increases the apparent affinity of anti-HIV antibodies by heteroligation. Nature *467*, 591–595.

Mouquet, H., Klein, F., Scheid, J.F., Warncke, M., Pietzsch, J., Oliveira, T.Y., Velinzon, K., Seaman, M.S., and Nussenzweig, M.C. (2011). Memory B cell antibodies to HIV-1 gp140 cloned from individuals infected with clade A and B viruses. PLoS ONE *6*, e24078.

Mouquet, H., Scharf, L., Euler, Z., Liu, Y., Eden, C., Scheid, J.F., Halper-Stromberg, A., Gnanapragasam, P.N., Spencer, D.I., Seaman, M.S., et al. (2012). Complex-type N-glycan recognition by potent broadly neutralizing HIV antibodies. Proc. Natl. Acad. Sci. USA *109*, E3268–E3277.

Muster, T., Steindl, F., Purtscher, M., Trkola, A., Klima, A., Himmler, G., Rüker, F., and Katinger, H. (1993). A conserved neutralizing epitope on gp41 of human immunodeficiency virus type 1. J. Virol. *67*, 6642–6647.

Pavri, R., and Nussenzweig, M.C. (2011). AID targeting in antibody diversity. Adv. Immunol. *110*, 1–26.

Pejchal, R., Doores, K.J., Walker, L.M., Khayat, R., Huang, P.S., Wang, S.K., Stanfield, R.L., Julien, J.P., Ramos, A., Crispin, M., et al. (2011). A potent and broad neutralizing antibody recognizes and penetrates the HIV glycan shield. Science *334*, 1097–1103.

Peled, J.U., Kuang, F.L., Iglesias-Ussel, M.D., Roa, S., Kalis, S.L., Goodman, M.F., and Scharff, M.D. (2008). The biochemistry of somatic hypermutation. Annu. Rev. Immunol. *26*, 481–511.

Pietzsch, J., Scheid, J.F., Mouquet, H., Klein, F., Seaman, M.S., Jankovic, M., Corti, D., Lanzavecchia, A., and Nussenzweig, M.C. (2010). Human anti-HIV-neutralizing antibodies frequently target a conserved epitope essential for viral fitness. J. Exp. Med. *207*, 1995–2002.

Rajewsky, K. (1996). Clonal selection and learning in the antibody system. Nature *381*, 751–758.

Reynaud, C.A., Garcia, C., Hein, W.R., and Weill, J.C. (1995). Hypermutation generating the sheep immunoglobulin repertoire is an antigen-independent process. Cell *80*, 115–125.

Scheid, J.F., Mouquet, H., Feldhahn, N., Seaman, M.S., Velinzon, K., Pietzsch, J., Ott, R.G., Anthony, R.M., Zebroski, H., Hurley, A., et al. (2009a). Broad diversity of neutralizing antibodies isolated from memory B cells in HIV-infected individuals. Nature *458*, 636–640.

Scheid, J.F., Mouquet, H., Feldhahn, N., Walker, B.D., Pereyra, F., Cutrell, E., Seaman, M.S., Mascola, J.R., Wyatt, R.T., Wardemann, H., and Nussenzweig, M.C. (2009b). A method for identification of HIV gp140 binding memory B cells in human blood. J. Immunol. Methods *343*, 65–67.

Scheid, J.F., Mouquet, H., Ueberheide, B., Diskin, R., Klein, F., Oliveira, T.Y., Pietzsch, J., Fenyo, D., Abadir, A., Velinzon, K., et al. (2011). Sequence and structural convergence of broad and potent HIV antibodies that mimic CD4 binding. Science *333*, 1633–1637.

Seaman, M.S., Janes, H., Hawkins, N., Grandpre, L.E., Devoy, C., Giri, A., Coffey, R.T., Harris, L., Wood, B., Daniels, M.G., et al. (2010). Tiered categorization of a diverse panel of HIV-1 Env pseudoviruses for assessment of neutralizing antibodies. J. Virol. *84*, 1439–1452.

Shibata, R., Igarashi, T., Haigwood, N., Buckler-White, A., Ogert, R., Ross, W., Willey, R., Cho, M.W., and Martin, M.A. (1999). Neutralizing antibody directed against the HIV-1 envelope glycoprotein can completely block HIV-1/SIV chimeric virus infections of macaque monkeys. Nat. Med. *5*, 204–210.

Simek, M.D., Rida, W., Priddy, F.H., Pung, P., Carrow, E., Laufer, D.S., Lehrman, J.K., Boaz, M., Tarragona-Fiol, T., Miiro, G., et al. (2009). Human immunodeficiency virus type 1 elite neutralizers: individuals with broad and potent neutralizing activity identified by using a high-throughput neutralization assay together with an analytical selection algorithm. J. Virol. *83*, 7337–7348.

Stanfield, R.L., Fieser, T.M., Lerner, R.A., and Wilson, I.A. (1990). Crystal structures of an antibody to a peptide and its complex with peptide antigen at 2.8 A. Science *248*, 712–719.

Thali, M., Moore, J.P., Furman, C., Charles, M., Ho, D.D., Robinson, J., and Sodroski, J. (1993). Characterization of conserved human immunodeficiency virus type 1 gp120 neutralization epitopes exposed upon gp120-CD4 binding. J. Virol. *67*, 3978–3988.

Tiller, T., Tsuiji, M., Yurasov, S., Velinzon, K., Nussenzweig, M.C., and Wardemann, H. (2007). Autoreactivity in human IgG+ memory B cells. Immunity *26*, 205–213.

Trkola, A., Purtscher, M., Muster, T., Ballaun, C., Buchacher, A., Sullivan, N., Srinivasan, K., Sodroski, J., Moore, J.P., and Katinger, H. (1996). Human monoclonal antibody 2G12 defines a distinctive neutralization epitope on the gp120 glycoprotein of human immunodeficiency virus type 1. J. Virol. *70*, 1100–1108.

Victora, G.D., and Nussenzweig, M.C. (2012). Germinal centers. Annu. Rev. Immunol. *30*, 429–457.

Wagner, S.D., Milstein, C., and Neuberger, M.S. (1995). Codon bias targets mutation. Nature *376*, 732.

Walker, L.M., Phogat, S.K., Chan-Hui, P.Y., Wagner, D., Phung, P., Goss, J.L., Wrin, T., Simek, M.D., Fling, S., Mitcham, J.L., et al.; Protocol G Principal Investigators. (2009). Broad and potent neutralizing antibodies from an African donor reveal a new HIV-1 vaccine target. Science *326*, 285–289.

Walker, L.M., Huber, M., Doores, K.J., Falkowska, E., Pejchal, R., Julien, J.P., Wang, S.K., Ramos, A., Chan-Hui, P.Y., Moyle, M., et al.; Protocol G Principal

Investigators. (2011a). Broad neutralization coverage of HIV by multiple highly potent antibodies. Nature *477*, 466–470.

Walker, L.M., Sok, D., Nishimura, Y., Donau, O., Sadjadpour, R., Gautam, R., Shingai, M., Pejchal, R., Ramos, A., Simek, M.D., et al. (2011b). Rapid development of glycan-specific, broad, and potent anti-HIV-1 gp120 neutralizing antibodies in an R5 SIV/HIV chimeric virus infected macaque. Proc. Natl. Acad. Sci. USA *108*, 20125–20129.

Wei, X., Decker, J.M., Wang, S., Hui, H., Kappes, J.C., Wu, X., Salazar-Gonzalez, J.F., Salazar, M.G., Kilby, J.M., Saag, M.S., et al. (2003). Antibody neutralization and escape by HIV-1. Nature *422*, 307–312.

Wilson, P.C., de Bouteiller, O., Liu, Y.J., Potter, K., Banchereau, J., Capra, J.D., and Pascual, V. (1998). Somatic hypermutation introduces insertions and deletions into immunoglobulin V genes. J. Exp. Med. *187*, 59–70.

Wu, T.T., and Kabat, E.A. (1970). An analysis of the sequences of the variable regions of Bence Jones proteins and myeloma light chains and their implications for antibody complementarity. J. Exp. Med. *132*, 211–250.

Wu, X., Yang, Z.Y., Li, Y., Hogerkorp, C.M., Schief, W.R., Seaman, M.S., Zhou, T., Schmidt, S.D., Wu, L., Xu, L., et al. (2010). Rational design of envelope identifies broadly neutralizing human monoclonal antibodies to HIV-1. Science *329*, 856–861.

Wu, X., Zhou, T., Zhu, J., Zhang, B., Georgiev, I., Wang, C., Chen, X., Longo, N.S., Louder, M., McKee, K., et al.; NISC Comparative Sequencing Program. (2011). Focused evolution of HIV-1 neutralizing antibodies revealed by structures and deep sequencing. Science *333*, 1593–1602.

Xiao, X., Chen, W., Feng, Y., and Dimitrov, D.S. (2009a). Maturation Pathways of Cross-Reactive HIV-1 Neutralizing Antibodies. Viruses *1*, 802–817.

Xiao, X., Chen, W., Feng, Y., Zhu, Z., Prabakaran, P., Wang, Y., Zhang, M.Y., Longo, N.S., and Dimitrov, D.S. (2009b). Germline-like predecessors of broadly neutralizing antibodies lack measurable binding to HIV-1 envelope glycoproteins: implications for evasion of immune responses and design of vaccine immunogens. Biochem. Biophys. Res. Commun. *390*, 404–409.

Zhou, T., Georgiev, I., Wu, X., Yang, Z.Y., Dai, K., Finzi, A., Kwon, Y.D., Scheid, J.F., Shi, W., Xu, L., et al. (2010). Structural basis for broad and potent neutralization of HIV-1 by antibody VRC01. Science *329*, 811–817.

EXTENDED EXPERIMENTAL PROCEDURES

Analysis of Antibody Framework Amino Acid Replacements versus CDR H3 Length

Antibodies with limited (Table S1A) and broad (Table S1B) neutralizing activity were analyzed for correlations between CDRH3 length and the number of amino acid replacements in the four framework regions (FWR1-4) in heavy chain only, light chain only, and both heavy and light chains. For the broad neutralizers, MPER antibody 10E8 (Huang et al., 2012) was added, and antibodies NIH45-46, 12A12, and 3BNC117 were excluded to avoid skewing of the data because these antibodies were closely related to VRC01, 12A21, and 3BNC60, respectively. The Spearman rank correlation coefficient was used for the analysis.

Analysis of Antibody Framework Amino Acid Replacements versus Interactive Surface Area on Antibody

The following antibodies with broad neutralization activity from Figures 2 and 3 were included in the structural analysis: VRC01 (PDB id: 3ngb [Zhou et al., 2010]), PGT128 (3tyg [Pejchal et al., 2011]), 4E10 (2fx7 [Cardoso et al., 2007]), 2G12 (1op5 [Calarese et al., 2003]), 2F5 (1tji [Ofek et al., 2004]), as well as 3BNC117, 12A21 (4jpv and 4jpw, unpublished data), PG16 (4dqo, unpublished data). In addition, structures of antibody-antigen complexes for the following antibodies were included: 10E8 (4g6f [Huang et al., 2012]), VRC-PG04 (3se9 [Wu et al., 2011]), F105 (3hi1 [Chen et al., 2009]), 17b (2nxy [Zhou et al., 2007]), 48D (3jwd [Pancera et al., 2010]), X5 (2b4c [Huang et al., 2005]), 447-52D (1q1j [Stanfield et al., 2004]), 2219 (2b1h [Stanfield et al., 2006]), 537-10D (3ghe [Burke et al., 2009]), D5 (2cmr [Luftig et al., 2006]), 412d (2qad [Huang et al., 2007]), 21c (3lqa [Diskin et al., 2010]), F425-B4e8 (2qsc [Bell et al., 2008]), as well as VRC-PG20 and VRC-CH31 (unpublished data). Antibodies NIH45-46 (3u7y [Diskin et al., 2011]), VRC03 (3se8 [Wu et al., 2011]), and PG9 (3u2s [McLellan et al., 2011]) were excluded to avoid skewing of the data because these antibodies were closely related to VRC01 and PG16. Interactive surface areas were computed using NACCESS (Hubbard and Thornton, 1993) and in-house scripts. The Spearman rank correlation coefficient was used for the analysis. The black line shown in Figure S4C was derived by linear regression of the values labeled in black.

SUPPLEMENTAL REFERENCES

Bell, C.H., Pantophlet, R., Schiefner, A., Cavacini, L.A., Stanfield, R.L., Burton, D.R., and Wilson, I.A. (2008). Structure of antibody F425-B4e8 in complex with a V3 peptide reveals a new binding mode for HIV-1 neutralization. J. Mol. Biol. *375*, 969–978.

Burke, V., Williams, C., Sukumaran, M., Kim, S.S., Li, H., Wang, X.H., Gorny, M.K., Zolla-Pazner, S., and Kong, X.P. (2009). Structural basis of the cross-reactivity of genetically related human anti-HIV-1 mAbs: implications for design of V3-based immunogens. Structure *17*, 1538–1546.

Cardoso, R.M., Brunel, F.M., Ferguson, S., Zwick, M., Burton, D.R., Dawson, P.E., and Wilson, I.A. (2007). Structural basis of enhanced binding of extended and helically constrained peptide epitopes of the broadly neutralizing HIV-1 antibody 4E10. J. Mol. Biol. *365*, 1533–1544.

Chen, L., Kwon, Y.D., Zhou, T., Wu, X., O'Dell, S., Cavacini, L., Hessell, A.J., Pancera, M., Tang, M., Xu, L., et al. (2009). Structural basis of immune evasion at the site of CD4 attachment on HIV-1 gp120. Science *326*, 1123–1127.

Diskin, R., Marcovecchio, P.M., and Bjorkman, P.J. (2010). Structure of a clade C HIV-1 gp120 bound to CD4 and CD4-induced antibody reveals anti-CD4 polyreactivity. Nat. Struct. Mol. Biol. *17*, 608–613.

Gonnet, G.H., Cohen, M.A., and Benner, S.A. (1992). Exhaustive matching of the entire protein sequence database. Science *256*, 1443–1445.

Huang, C.C., Tang, M., Zhang, M.Y., Majeed, S., Montabana, E., Stanfield, R.L., Dimitrov, D.S., Korber, B., Sodroski, J., Wilson, I.A., et al. (2005). Structure of a V3-containing HIV-1 gp120 core. Science *310*, 1025–1028.

Huang, C.C., Lam, S.N., Acharya, P., Tang, M., Xiang, S.H., Hussan, S.S., Stanfield, R.L., Robinson, J., Sodroski, J., Wilson, I.A., et al. (2007). Structures of the CCR5 N terminus and of a tyrosine-sulfated antibody with HIV-1 gp120 and CD4. Science *317*, 1930–1934.

Hubbard, S., and Thornton, J. (1993). NACCESS. Computer Program (London: Department of Biochemistry and Molecular Biology, University College London).

Luftig, M.A., Mattu, M., Di Giovine, P., Geleziunas, R., Hrin, R., Barbato, G., Bianchi, E., Miller, M.D., Pessi, A., and Carfí, A. (2006). Structural basis for HIV-1 neutralization by a gp41 fusion intermediate-directed antibody. Nat. Struct. Mol. Biol. *13*, 740–747.

McLellan, J.S., Pancera, M., Carrico, C., Gorman, J., Julien, J.P., Khayat, R., Louder, R., Pejchal, R., Sastry, M., Dai, K., et al. (2011). Structure of HIV-1 gp120 V1/V2 domain with broadly neutralizing antibody PG9. Nature *480*, 336–343.

Ofek, G., Tang, M., Sambor, A., Katinger, H., Mascola, J.R., Wyatt, R., and Kwong, P.D. (2004). Structure and mechanistic analysis of the anti-human immunodeficiency virus type 1 antibody 2F5 in complex with its gp41 epitope. J. Virol. *78*, 10724–10737.

Pancera, M., Majeed, S., Ban, Y.E., Chen, L., Huang, C.C., Kong, L., Kwon, Y.D., Stuckey, J., Zhou, T., Robinson, J.E., et al. (2010). Structure of HIV-1 gp120 with gp41-interactive region reveals layered envelope architecture and basis of conformational mobility. Proc. Natl. Acad. Sci. USA *107*, 1166–1171.

Stanfield, R.L., Gorny, M.K., Williams, C., Zolla-Pazner, S., and Wilson, I.A. (2004). Structural rationale for the broad neutralization of HIV-1 by human monoclonal antibody 447-52D. Structure *12*, 193–204.

Stanfield, R.L., Gorny, M.K., Zolla-Pazner, S., and Wilson, I.A. (2006). Crystal structures of human immunodeficiency virus type 1 (HIV-1) neutralizing antibody 2219 in complex with three different V3 peptides reveal a new binding mode for HIV-1 cross-reactivity. J. Virol. *80*, 6093–6105.

Zhou, T., Xu, L., Dey, B., Hessell, A.J., Van Ryk, D., Xiang, S.H., Yang, X., Zhang, M.Y., Zwick, M.B., Arthos, J., et al. (2007). Structural definition of a conserved neutralization epitope on HIV-1 gp120. Nature *445*, 732–737.

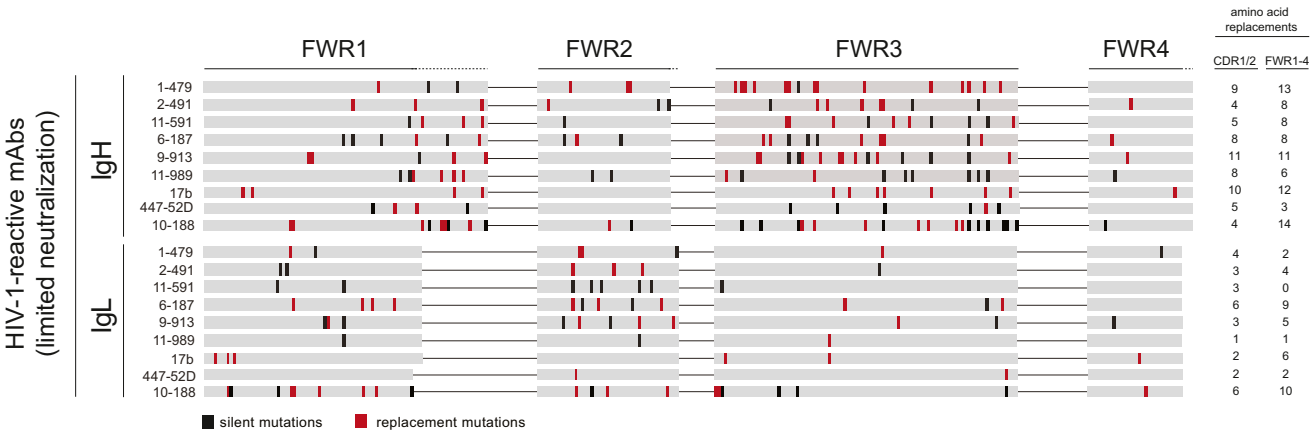

Figure S1. FWR Mutations in HIV-1-Reactive Antibodies with Limited Neutralizing Activity, Related to Figure 1

Position of FWR mutations in heavy and light chain of 9 investigated antibodies with limited neutralizing activity. Indicated are silent (black) mutations and replacement (red) mutations. Number of replacement mutations within CDR1/2 and FWR1-4 are listed in the two columns at the very right. For 17b only amino acid changes (red) are shown.

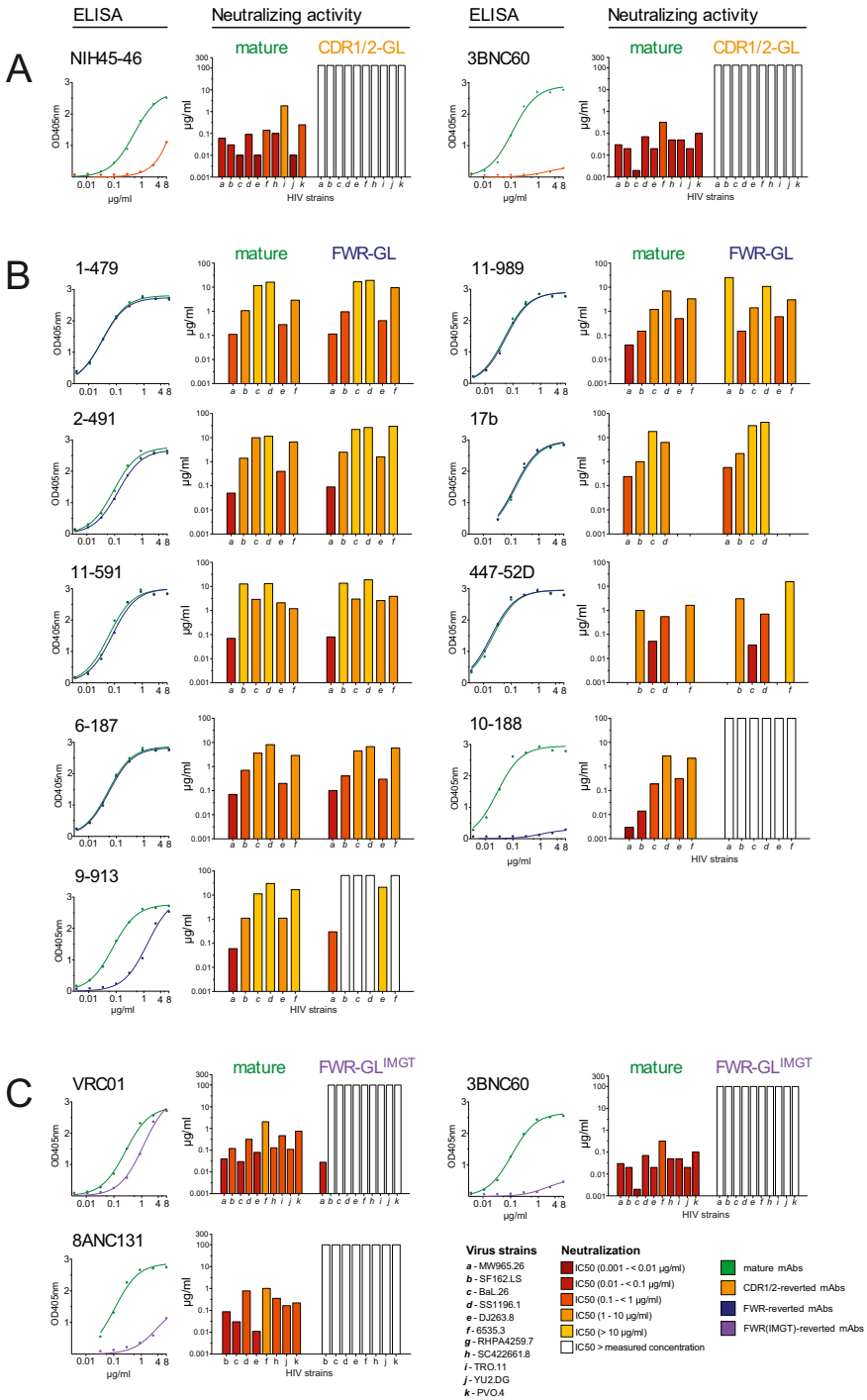

Figure S2. Binding and Neutralization Activity of Mature, CDR1/2-GL, FWR-GL and FWR-GL^{IMGT} Antibodies, Related to Figure 2

(A–C) Binding to gp140^{YU2} (ELISA; left) and neutralization activity (right) of mature antibodies (green) and (A) antibodies with CDR1 and CDR2 reverted to germline (CDR1/2-GL; orange); (B) antibodies with limited neutralization activity and FWRs reverted to germline (FWR-GL, blue) and (C) antibodies with FWRs reverted to germline according to IMGT alignment (FWR-GL^{IMGT}, purple). Neutralization panels on the right compare IC_{50} values for neutralization of Tier 1 (MW965.26, SF162.LS, Bal.26, SS1196.1, DJ263.8, 6535.3) Tier 2 (RHPA4259.7, SC422661.8, TRO.11, YU2.DG), and Tier 3 (PVO.4) viruses. Neutralization activity is color coded (dark red, IC_{50} below 0.01 µg/ml; red, 0.01–<0.1 µg/ml; orange, 0.1–<1 µg/ml; light orange, 1–10 µg/ml; yellow: >10 µg/ml; white, IC_{50} was not achieved up to the tested concentration).

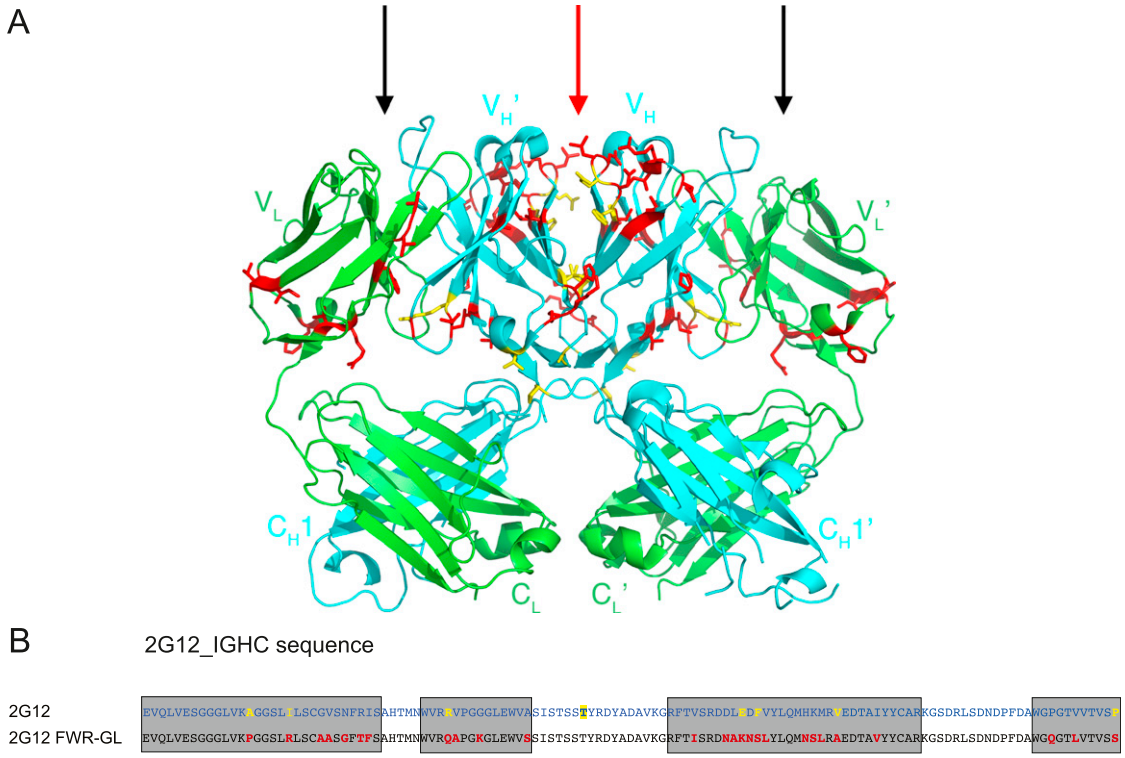

Figure S3. Illustration of Mutations in 2G12 Responsible for Domain Swapping, Related to Figure 2

(A) Ribbon representation of the domain swapped $(Fab)_2$ of 2G12 (PDB code 1OP3). Somatically mutated FWR residues are highlighted in red and yellow, with yellow representing residues that were shown to be important for domain swapping (Huber et al., 2010). Black arrows point to canonical antigen combining sites located at the V_H-V_L interface of each Fab. Red arrow points to an additional antigen-binding site formed at the V_H-V_H' interface (Calarese et al., 2003).

(B) Amino acid sequence of 2G12 and 2G12 FWR-GL. Residues implicated in domain swapping are highlighted in yellow. FWRs and FWR mutations are highlighted in gray and red, respectively.

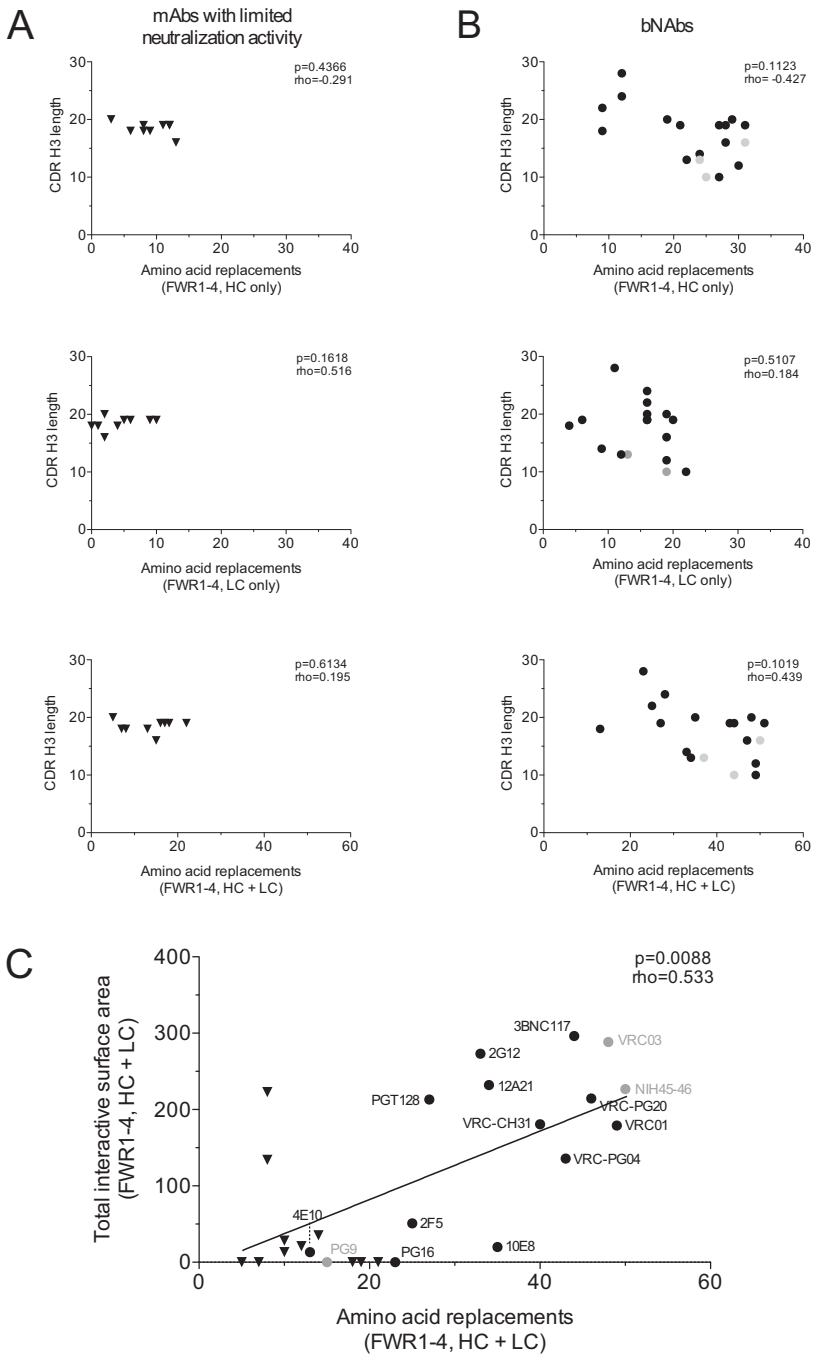

Figure S4. Relationships between Framework Amino Acid Replacements and Both Antibody CDRH3 Length and Interactive Surface Area

(A and B) Each symbol represents one HIV-1-directed antibody with limited (triangles) or broad (dots) neutralization activity. No significant correlation (Spearman) was observed for either limited (A) or broad (B) neutralizers when comparing CDRH3 lengths against FWR1-4 amino acid replacements in heavy chain only, light chain only, or both heavy and light chains.

(C) Relationship between antibody interactive surface area and framework amino acid replacements. A significant correlation (Spearman) was observed between the total interactive surface area and the number of amino acid replacements in FWR1-4 for a set of 23 HIV-1-directed antibodies with known antibody-antigen structures. In order to avoid skewing NIH45-46, VRC03, and PG9 (gray dots) were excluded from analysis because these mAbs are clonal members of the included mAbs VRC01 and PG16.

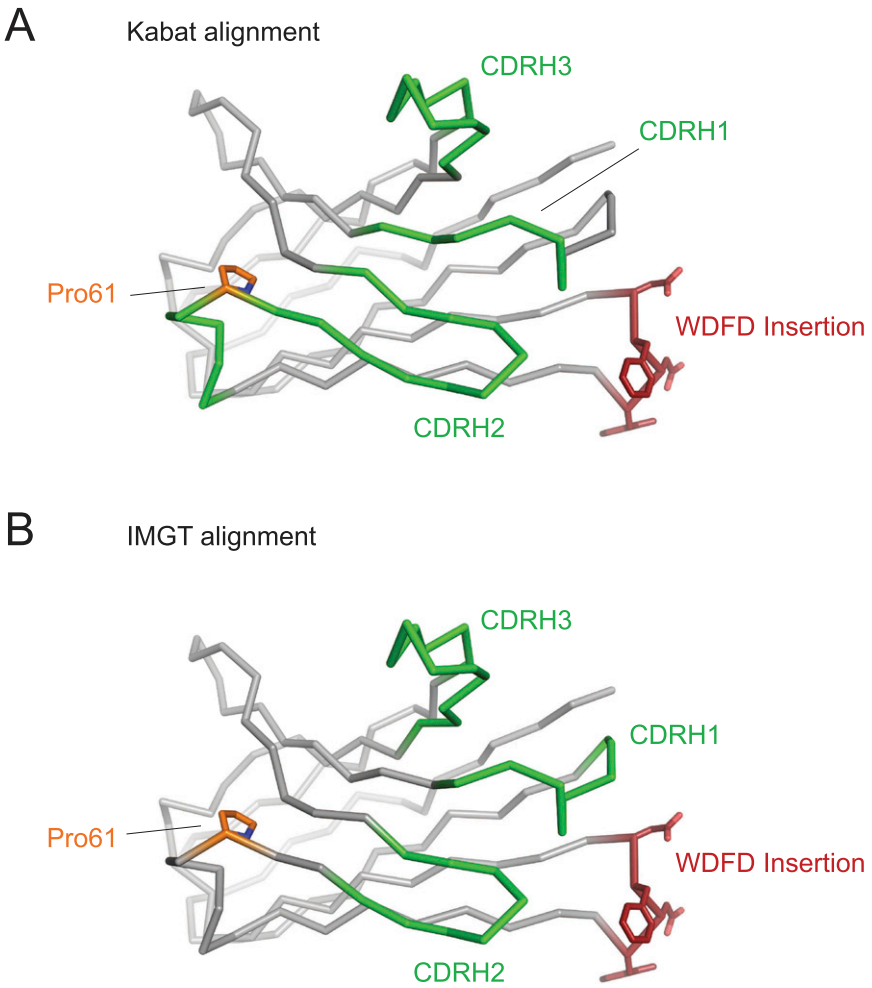

Figure S5. Structure of the V_H Domain of 3BNC117 in Its gp120-Bound Conformation, Related to Figure 4

(A and B) gp120-bound 3BNC117 IGVH with CDRs highlighted in green and FWRs in gray as assigned by Kabat (A) and IMGT (B). The side chains of Pro61 (orange) and the 3BNC60 WDFD insertion (red) are highlighted. Pro61 and nearby residues (59–65) differ in the structure of free 3BNC60 due to a crystal contact involving this region (Scheid et al., 2011).

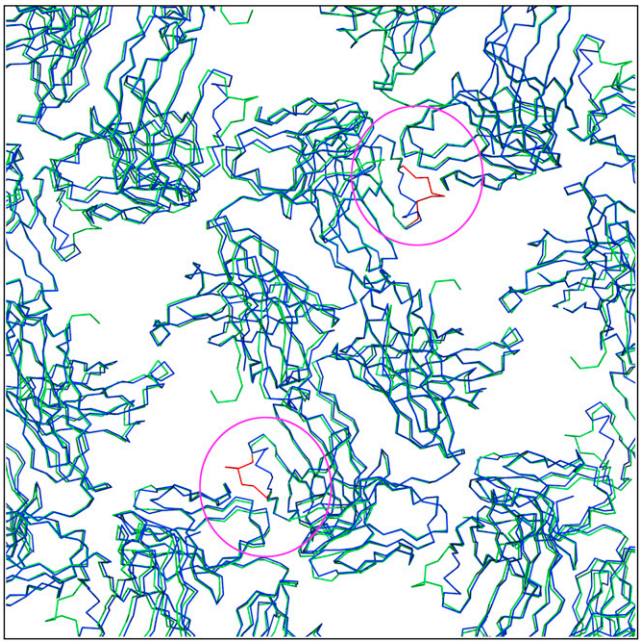

Figure S6. Overview of the Packing in Crystals of 3BNC60 and 3BNC60^{P61A}, Related to Figure 6

3BNC60 (green) and 3BNC60^{P61A} (blue) crystallized in the same space group utilizing nearly identical crystal packing interactions. Residues 59–65 of 3BNC60 (red), which deviate from the canonical variable domain fold, contribute to packing interactions in the 3BNC60 crystals (pink ovals). Although the 3BNC60^{P61A} crystal packing is almost identical, the extra hydrogen bond that Ala61 forms with the C' β strand (Figure 6A) prevents residues 59–65 of 3BNC60^{P61A} from adopting a similar conformation and interacting with a crystallographic neighbor.